UNIVERSITY OF UDINE

PHD COURSE IN MOLECULAR AND CELLULAR MEDICINE (XXIX CYCLE)

Department of Medical and Biological Sciences

SIZE-DEPENDENT INTERNALIZATION OF EXOSOMES

PhD STUDENT:
Caponnetto Federica

SUPERVISOR:
Prof. Carla di Loreto

ASSISTANT SUPERVISORS:
Dott.ssa Daniela Cesselli
Prof. Enrico Ferrari

YEAR OF FINAL EXAM 2017

1 SUMMARY

ABSTRACT 4
1 INTRODUCTION 6
1.1 GLIOMAS AND GLIOMA ASSOCIATED STEM CELLS 6
1.1.1 GENERAL OVERVIEW OF THE PATHOLOGY 7
1.1.2 PRECISION MEDICINE AND THE IMPORTANCE OF THE TUMOR MICROENVIRONMENT 10
1.2 EXOSOMES 16
1.2.1 EXOSOME GENERAL FEATURES, CONTENT AND FUNCTION 17
1.2.2 THE ELUSIVE NATURE OF EXOSOMES: ISSUES ON EXTRACTION AND QUANTIFICATION METHODS 24
2 AIM OF THE STUDY 35
3 MATERIALS AND METHODS 36
3.1 CELL CULTURE 36
3.1.1 Primary and commercial cell lines 36
3.2 EXOSOME ISOLATION 37
3.2.1 Ultracentrifugation 37
3.2.2 ExoQuick precipitation 37
3.3 EXOSOME SIZE ANALYSIS 37
3.3.1 Atomic force microscopy 37
3.3.2 Nanoparticle Tracking Analysis 38
3.4 EXOSOME QUANTIFICATION 38
3.5 EXOSOME UPTAKE 39
3.5.1 Confocal and epifluorescence imaging 39
3.5.2 Flow cytometry 39
3.6 FUNCTIONAL ASSAY 40
3.7 STATISTICS 40
4 RESULTS 41
4.1 DIFFERENT PURIFICATION TECHNIQUES AFFECT THE SIZE DISTRIBUTION OF THE EXOSOMIAL PREPARATIONS 41
4.2 THE CONTRIBUTION OF THE PURIFICATION TO UC AND EQ PREPARATIONS 47
4.3 MOLECULAR ASSAYS ON EQ AND UC EXOSOMES 49
4.4 A172 CELLS PREFERENTIALLY UPTAKE PARTICLES PURIFIED BY EXOQUICK PRECIPITATION 52

4.5 THE EFFECTS OF EXOSOMES' DIFFERENTIAL UPTAKE ON FUNCTIONAL ASSAYS 59
5 DISCUSSION 62
6 BIBLIOGRAPHY 67

ABSTRACT

Exosomes are biologically active extracellular vesicles, whose size range from 30 to 100nm, which are released by many cell types in various body fluids. These particles have been proved to be strong players in cell-cell communication, thus reaching interest especially about their involvement in cancer progression, invasion and metastasis. For example, our group has already investigated the tumor supporting function of exosomes released by Glioma-Associated Stem Cells (GASC).

Considering the mechanism of action of exosomes, besides the undeniable role exerted by the message they deliver, much interest is now focused on to their physical properties, since they could also influence the biological function observed, as shown for bioengineered nanoparticles, and consequently their therapeutic potential.

As exosomal size is nanoscopic, the estimation of particle size and density has been elusive, and the use of several techniques has been applied, such as Transmission Electron Microscopy (TEM), Atomic Force Microscopy (AFM), Nanoparticle Tracking Analysis (NTA) and Dynamic Light Scattering (DLS), each displaying strength and weaknesses. Moreover, another extremely relevant matter, for which it has not yet reached a consensus, regards the ideal method to isolate exosomes, as it could lead to different exosomal populations with different features.

In this thesis, we compared the exosomes preparations obtained by two different enrichment methods, wondering if this could affect the exosome uptake by cells and their ability to alter the biological functions of target cells. Therefore, we isolated exosomes released by patient-derived high-grade GASC and human glioblastoma cell line A172 in cell supernatants using both ultracentrifugation (UC) and ExoQuick (EQ) precipitation methods. Then we assessed the purified particles both for their physical properties (characterizing particle size and particle density) using AFM and NTA, and molecular properties (evaluating total protein content and a specific exosomal marker) using Bradford, BiCinchoninic Acid Assay (BCA) and CD9 ELISA assay. Then we performed cell uptake assays to observe the differential internalization of the preparations, and finally we evaluated whether this differential internalization could influence glioma cell motility.

Our results demonstrate that polymer-based precipitation results in particles that have a size distribution smaller than that of ultracentrifuge-isolated ones. Moreover, we further established that smaller exosomes are better uptaken by the receiving cells and, furthermore, this affects cell motility.

These data suggest that the isolation method could profoundly affect the size distribution of the obtained exosomal preparation and this is associated with differences in their physical and biological properties, thus improving or decreasing their potential therapeutic capability.

1 INTRODUCTION

1.1 GLIOMAS AND GLIOMA ASSOCIATED STEM CELLS

Gliomas are the most common neuroepithelial tumor type and account for the 77% of all human brain tumors [1,2]. Based on World Health Organization classification, the most malignant form of glioma is grade IV, which includes the glioblastoma multiforme (GBM), which represents the most aggressive extremity of the diffuse astrocytoma spectrum [2]. Unfortunately, GBM is also the most common astrocytic pathology and its average incidence rate is 2-3 per 100.000 people [2]. The median overall survival of these lethal tumors is around 15-18 months and less than 3% of the patients survive 5 years after diagnosis [2].

Gliomas possess a very heterogeneous range of phenotypes that makes challenging their clinical management [1]. Currently, wide genome studies have been conducted to better characterize gliomas[3,4]. Although many progresses have been made in the prognostic stratification of patients and in the identification of novel biomarkers, no hints about possible innovative therapeutic strategies have been obtaining. Thus, this fatal cancer still needs further exploring [3,4]. For this reason, much attention has been directed not only to the genetic changes occurring in the tumor initiating cells, but also to glioma tumor microenvironment [5–7]. This latter has recently arisen much attention in the attempt to dissect "messages" and interaction pathways with the tumor cells. In fact, it has already been assessed that the microenvironment plays a key role in tumor proliferation, invasion, aggressiveness and metastasis. It is therefore important to exploit the "cross-talk" between the tumor initiating cells and the tumor microenvironment to identify novel target opportunities [5–7].

This section will focus on the general overview of the pathology, reporting the epidemiology, etiology, histopathology diagnosis and therapy of this aggressive neoplasia. Moreover, there will be a section focusing on the tumor microenvironment and its role in cancer progression. Finally, we will introduce the Glioma Associated Stem Cells, GASCs. This population is constituted of activated mesenchymal stem cells representative of the glioma microenvironment, since able to increase the glioma aggressiveness through the release of extracellular vesicles, named exosomes, which we will be further explored in the sequent section.

1.1.1 GENERAL OVERVIEW OF THE PATHOLOGY

Glioblastoma represents a neoplasia characterized by poor prognosis, with a median survival of only 14–16 months, despite a multimodal treatment including surgery, cytotoxic chemotherapy and radiation [1,3]

Since 1950s, the classification of tumors of the Central Nervous System (CNS) was based merely on the histologic evaluation, possible through histochemical analysis such as hematoxylin-eosin staining, able to suggest the tumor cell of origin, differentiation levels, presence of infiltration/necrosis and the vascularization of the tumor tissue [2,9]. Further improvements were made in the classification of gliomas through the introduction of the immunohistochemical detection of Glial Fibrillary Acidic Protein (GFAP), antigen KI67/E3 ubiquitin-protein ligase MIB1 (Mib-1), tumor suppressor protein p53, and later on Isocitrate DeHydrogenase (IDH) [1,2]. Recently, as the new diagnostic scenario has shifted toward biomolecular investigations to stratify gliomas, new routine analyses, such as Fluorescent *In situ* Hybridization (FISH) to verify 1p19q co-deleted genotype and molecular investigations on the O6-alkylguanine DNA alkyltransferase (MGMT) methylated status and Epidermal Growth Factor Receptor (EGFR) amplification, have been introduced [1,2]. These new assays are not only able to better stratify glioma patients, but add molecular parameters to the previous WHO classification of CNS tumors and glioblastomas [1,2].

According to the 2016 CNS WHO classification, glioblastomas are now divided in tree main variants:

- IDH-wild type GBM → generally defined as primary GBM, is the most frequent tumor subtype (almost 90% of cases) and has a late onset (over 55 years)
- IDH-mutant GBM → generally called secondary glioblastoma, is compatible with lower grade gliomas that underwent progression; is less frequent (10% of cases) and with an earlier onset with respect to IDH-wild type GBM
- Not otherwise specified (NOS) GBM → GBM where IDH mutation couldn't be assessed

The differences between IDH wildtype and IDH mutant glioblastomas are indicated in Table 1.

Table 1 Key characteristics of IDH-wildtype and IDH-mutant glioblastomas. From Louis et al. 2016

	IDH-WILDTYPE GLIOBLASTOMA	IDH-MUTANT GLIOBLASTOMA
SYNONYM	PRIMARY GLIOBLASTOMA, IDH-WILDTYPE	SECONDARY GLIOBLASTOMA, IDH-MUTANT
PROPORTION OF GBM	90%	10%
MEDIAN AGE AT DIAGNOSIS	AROUND 62 YEARS	AROUND 44 YEARS
MALE TO FEMALE RATIO	1.42:1	1.05:1
MEDIAN LENGTH OF CLINICAL HYSTORY	4 MONTHS	15 MONTHS
MEDIAN OVERALL SURVIVAL SURGERY+RADIOTHERAPY SURGERY+RADIOTHERAPY+CHEMOTHERAPY	 9.9 MONTHS 15 MONTHS	 24 MONTHS 31 MONTHS
TERT PROMOTER MUTATIONS	72%	26%
TP53 MUTATIONS	27%	81%
ATRX MUTATIONS	EXCEPTIONAL	71%
EGFR AMPLIFICATION	35%	EXCEPTIONAL
PTEN MUTATIONS	24%	EXCEPTIONAL

Recently the lack of effective treatment for these pathologies has been attributed to the newest concept of glioblastoma as a "molecularly heterogeneous disorder" [1,3]. This realization induced researchers to look deeper into the molecular landscape of these tumors, trying to understand and profile the pathology[10]. The Cancer Genome Atlas (TCGA) attempted a classification of the molecular variants present in GBM, thus stratifying this tumor in four molecular subclasses. Based on the genomic, epigenomic and transcription profile, these four classes were referred as neural, proneural, classical and mesenchymal [11]. Figure 1.1 displays the epigenetic classification of GBM that comprehends six classes, instead.

Even though it is not yet clear whether this classification can have an impact on the current therapeutic strategies, the future direction is to take advantage of molecular analyses not only to improve the prognostic stratification of the patients but to develop optimal and targeted treatments in a precision medicine approach [1].

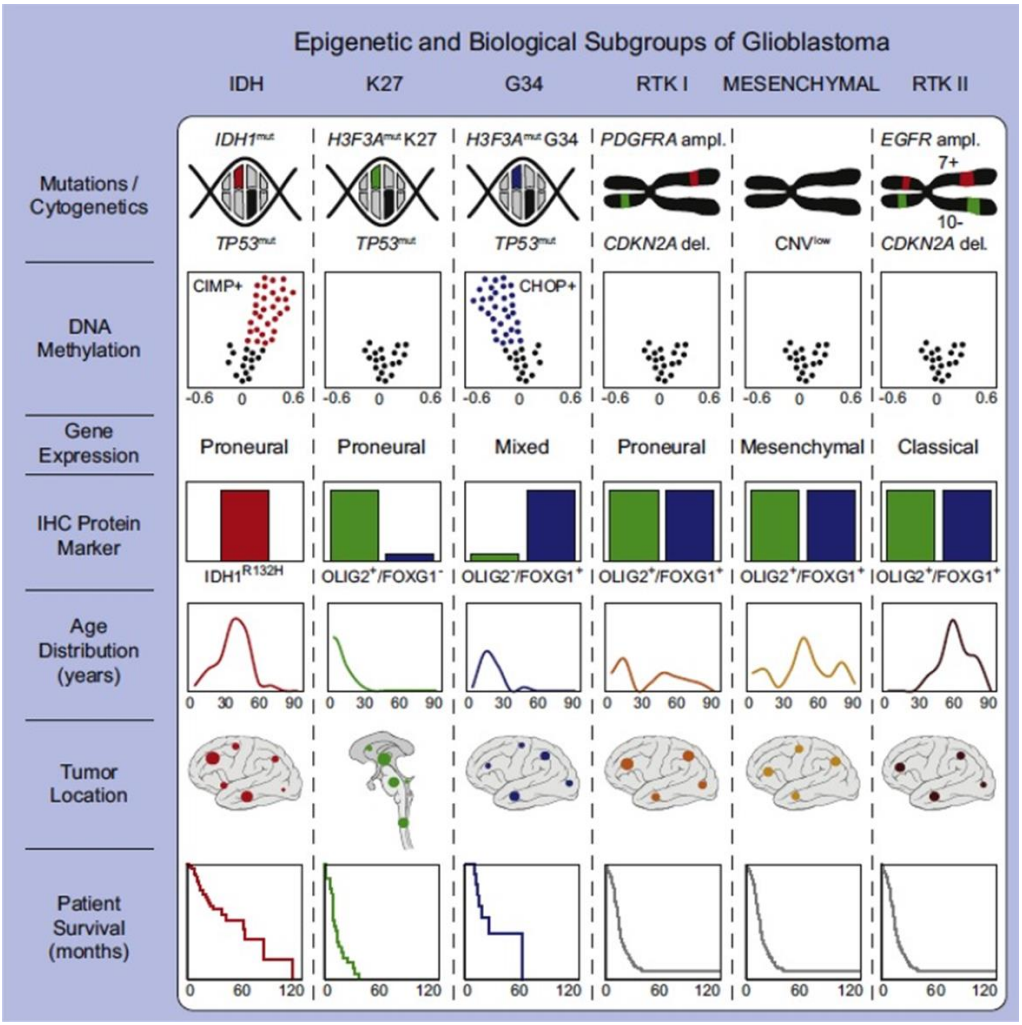

Figure 1.1 Graphical summary of key molecular and biologic characteristics of glioblastoma subgroups. From Weathers and Gilbert, 2014.

GLIOBLASTOMA TREATMENT

Glioblastomas, being the most aggressive form of glioma, despite an aggressive treatment still possess an extremely poor prognosis [1,12–14]. Multimodal approaches are actually employed in the treatment of this neoplasia. Up to these days, the management of glioblastoma patients includes radical surgery, fractionated beam photon radiation and chemotherapy using temolozomide (TMZ) [15,16]. Despite the best efforts, this therapy could improve the median overall survival of not more than 10 months, pushing researches into assessing new putative targets to be tested in clinical trials and in defining new biomarkers able to support the decision-making process. As explained above, genomic analyses are providing interesting insights on potential innovative

therapies [1,17]. Moreover, antiangiogenic therapies and immunotherapy are now under evaluation in several clinical trials [1,3,18].

Regarding anti-angiogenic treatments, results have not been encouraging but it is undeniable that the exploitation of the pathways through which angiogenesis inhibitors act might be fundamental for a better understanding of tumor growth and drug-resistance processes. This knowledge could permit us to include antiangiogenic agents in the present therapies as a support to the current state-of –the-art treatments.

More comforting are the results obtained through immunotherapy, and for this reason, more and more trials are being currently developed and devised [3,14,19–21].

1.1.2 PRECISION MEDICINE AND THE IMPORTANCE OF THE TUMOR MICROENVIRONMENT

In January 2015, U.S.A President Obama introduced a new initiative termed Precision Medicine approach [22].

This model implies shaping therapies and treatments accordingly to specific biomolecular peculiarities of the patient. This approach relies on the ability to stratify patients in subpopulations, which differ from each other for biological or molecular features that can affect their response to treatments and prognosis [22]. This way, specific therapies could be administered to specific classes of patients, sparing side effects and expenses to those who could not benefit from it. In this new concept the keywords are "stratification" and "subpopulations", which means that precision medicine is not personalized (i.e. tailored to the individual patient), but aims at finding, on the basis of several epidemyologic, clinical and biomolecular features, homogeneous subgroups of patients that share common prognostic markers and/or response to therapy [22]. Since glioblastoma, as previously explained, is a pathology that shows a heterogeneous clinical behavior, it is safe to say that this new initiative could fit well in the precision medicine scenario [22].

In the search of prognostic markers, recent studies identified hallmarks that not only belonged to the actual tumor cells, but also to the tumor microenvironment (TME) surrounding and communicating with these cells, which raised much attention [5,6,23]. This

concept was first addressed in the late 1970s by Haddow and Dvorak that referred to tumors as "non-healing wounds", thus reconsidering the hypothesis of tumor cells as the only key players in the tumor establishment [24]. Later, in the 2000s, Hanahan and Weinberg remarked the idea of the tumor niche as a dynamic entity in which different cell types and molecules are involved in a harmful cross talk that results in tumor initiation and progression [25]. The term microenvironment refers to all cells (e.g. blood vessels, immune cells and fibroblasts), vesicles and molecules that surround tumor cells and interact with them, as well as to the extracellular matrix [23,26,27]. In numerous solid tumors, the TME cells have been reported as fundamental in tumor progression, resistance and metastasis, even though the origin of these tumor-supporting cells is still unclear (from resident cells that are activated to bone marrow cells that migrate toward the tumor site) as well as the mechanisms of their activation (possibly epigenetic) [5,23]. It is increasing the knowledge that glioma stem cells (GSC) and the tumor niche are continuously modeling and influencing each other in a dynamic cross talk [6,28]. Gliomagenesis and glioma progression is no exception to this topic, thus many authors revealed the endless and extended interaction between glioma stem cells and the glioma microenvironment as an important player in the development of the pathology [6,28]. Up to now, two specialized niches have been identified in the glioma microenvironment as possible preservers of the GSC self-renewal ability, the vascular and the hypoxic niche [18,31–33]. In addition, vascular cells, microglia, peripheral immune cells, activated astrocytes and neural precursor cells are being studied as important players in the pathologic progression. For these reasons, the study of the glioma microenvironment could provide powerful insights on new molecular targets that lead to new therapies for the "treatment" of the microenvironment [18,31–33].

In fact, the TME, through the release of trophic factors and enzymes, is able to influence GSC that, on the other hand, could signal to the TME promoting immune escape, resistance and invasion.

Moreover, many stroma elements of the TME have been revealed as strong predictive and prognostic markers, thus leading to new potential therapeutic targets, which are currently being investigated [5,23,27]. One of the benefits of targeting the TME instead of the GSCs is that TME cells are fairly genetically stable, thus easier to study and less prone to develop resistance to treatments.

To summarize, the tumor-associated stroma acts as an active player in tumorigenesis and contributes to tumor progression by sustaining tumor proliferation, inducing angiogenesis, avoiding immune destruction, deregulating cellular energetics, inducing invasion and metastasis [29,30].

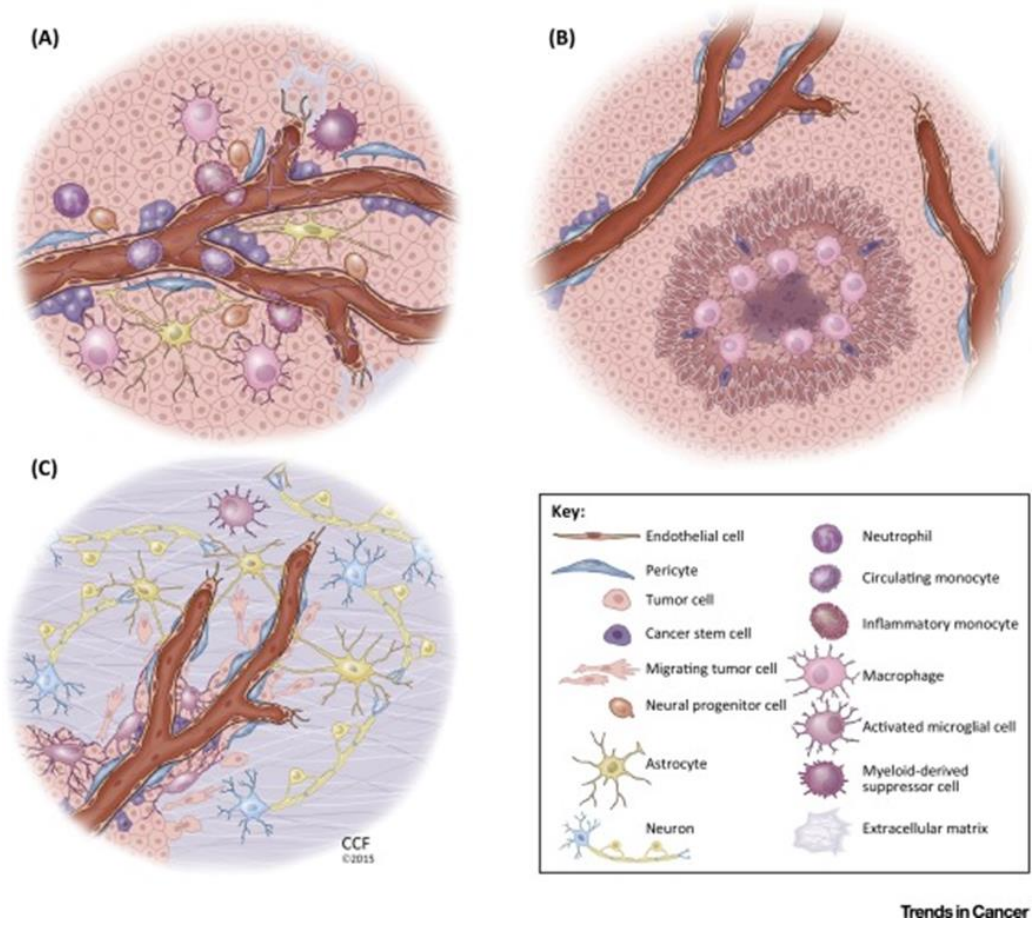

Figure 1.2 The perivascular (A), hypoxic (B) and invasive (C) GBM niche. From Hambardzumyan and Bergers, 2015.

THE THERAPEUTIC OPPORTUNITY

As already described above, the TME constitutes a very interesting target to exploit for tumor therapy and treatment [5,23]. In fact the TME, unlike the genetically instable GSCs, can be less prone to develop drug resistance. For this reason, attention has shifted to therapies directed to the TME and its cross talk with the tumor cells, encouraging the development of novel clinical trials [5,23].

As the contribution of the TME to cancer can be either pro-tumorigenic or, at least in the initial phase of tumor development, oncosuppressive, the new frontier is, instead of ablating the tumor-TME cross talk, to "re-educate" the TME to send specific antitumorigenic messages. In this way, the TME cure could become the keystone for the disruption of the tumor itself[7].

In this regard, the development of *in vitro* culture models of the glioma microenvironment could be an essential step to better assess the biological and molecular features of TME [5,23] (see next paragraph). This could be important either to study specific therapies aimed at blocking the activation of the TME or its communication with cancer cells or to search for novel diagnostic, prognostic and predictive markers. Next step would be the development of *in vivo* models of pathology strictly resembling the human tumor to directly assess the in vivo efficacy of putative drugs [5,23].

GASC ARE A POPULATION OF STEM CELLS WITH TUMOR- SUPPORTING FUNCTION

Our laboratory developed a novel approach to efficiently isolate and culture multipotent adult stem cells from different adult tissues, such as heart, bone marrow and liver [34–36]. Applying this protocol to gliomas, we were able to obtain a population of cells that were not tumor initiating, but had stem properties as well as tumor supporting features [37]. This achievement lead us to the idea that we could efficiently isolate mesenchymal stem cells associated with the glioma microenvironment. For this reason, we named these cells Glioma Associated Stem Cells, or GASC. Since 2006, more than 300 glioma samples, both from high-grade and low-grade gliomas, were isolated with this protocol and, despite the stringent culture conditions, almost 300 cell cultures were established. Moreover, we demonstrated that these cell lines matched the International Society for Cellular Therapy criteria required to be defined mesenchymal stem cells for their immunophenotype and functional features [37]. These multipotent cells could be easily propagated in culture and maintain an activated phenotype. Table 2 gathers all the GASC properties and through which assays they were assessed. Specifically, *in vitro* experiments were performed to assess the stem cell phenotype, clonogenicity and multipotency [37].

Table 2. Summarized features of GASC cells. From Bourkoula et al. 2014.

MORPHOLOGY	Fibroblast-like morphology, confirmed by the expression of mesenchymal cell markers (CD90, CD73, CD105)
UNDIFFERENTIATED PHENOTYPE	Expression of pluripotent state specific transcription factors (OCT-4, Nanog, Sox-2) as well as of early intermediate filaments (Vimentin e Nestin).
CLONOGENICITY	Elevated clonal self-renewal and maintenance of an undifferentiated state.
MULTIPOTENCY	Ability to differentiate through the neural (neuronal, glial and oligodendrocytic cells), mesodermic and endodermic lineages.
PRO-TUMORAL ABILITY	High anchorage-independent growth ability and pro-aggressive behavior on tumoral cell lines through the release of exosomes

All data confirmed that this *in vitro* model represented the activated glioma microenvironment, and led us to explore whether it could be used to predict patient prognosis [37]. Indeed, GASC surface markers were able to prognostically stratify patients since they correlated with both patient overall survival and malignant progression free survival [37]. This ultimate data supported the bounty of this *in vitro* patient-based model and the possibility to use it to customize healthcare in a precision medicine approach.

In order to find putative targets that could be exploited for novel therapeutic strategies, besides describing the peculiar features of GASC, attention has been subsequently focused on understanding how these cells exerted their tumor supporting function, [37].

In this regard, we showed that GASC interact with tumor cells by modulating their adhesive properties and releasing "messages" under the form of exosomes [37,38].

The first property of GASC was assessed using sophisticated methods of Atomic Force Microscopy and elastic module algorithms. We verified that GASC cells, not only have a harder texture than GSC, but are also able to modify the adhesive properties of glioblastoma cells. This reveals that studying cell adhesion and elasticity could uncover interesting phenomena in the GASCs-GSCs interaction [38].

Another attractive field of study is the interaction between the microenvironment and glioma stem cells through the release of extracellular vesicles, among which exosomes represent an interesting topic of research [37]. As described below, these particles are 30-100 nm nanovesicles that are released from many cell types in many body fluids sending messages under the form of their molecular "cargo" constituted by DNA, RNAs, mRNAs, microRNAs and proteins [39]. For this reason, these vesicles are considered important players in the intercellular communication [39]. One of the first laboratories demonstrating the potential of these particles on the glioma setting was the one of Breakefield, who not only demonstrated that glioblastoma cells release exosomes, that contain pro-tumorigenic messages, but also that they can affect neighbor as well as distant cells through the bloodstream [40]. Regarding the TME, similarly to what shown in breast tumors, were exosomes released from tumor-associated fibroblasts have been revealed to induce a metastatic phenotype in breast tumor [41], GASC exosomes were able to support the tumor growth by increasing the biological aggressiveness of both commercial glioblastoma cell lines and patient-derived GSC.

1.2 EXOSOMES

Research has always focused its attention on the mechanisms that undergo intercellular communication. In fact, much literature has been published on cell-cell contact or exchange of molecules, such as lipids, proteins and nucleotides [42–44].

For this reason, since in the 1980s extracellular vesicles (EV) have been discovered as a powerful tool for cell-cell communication, increasing interest has been addressed in that direction. The key of their peculiarity is their outer composition, as it is constituted of a phospholipid bilayer (compatible to one of which cells are composed) [45].

Since the beginning, EV have been sub-classified in different classes (e.g. microvescicles, oncosomes, exosomes, ectosomes, apoptotoic bodies) based on their biogenesis, origin, composition and function. Although the classification is still under implementation, there is a class of these vesicles, which is actually being intensively studied, whose literature, in the last 10 years, has been multiplied almost twenty times. These vesicles, named exosomes, are still under deep investigation, but the scientific community agrees in the importance of these particles in cell-cell communication [39,42]. Although they are being thoroughly investigated just in these past 10 years, Johnstone et al. first reported their existence in 1983, as vesicles obtained from reticulocytes' culture media [45].

This chapter will firstly present a general identikit of these vesicles (Figure 1.3), describing their content and functions, especially in gliomas, which makes them so intriguing. Then we will proceed with the description of the current issues concerning the manipulation of these particles, from the isolation to the quantification, describing each available method and trying to speculate about the putative best isolation and quantification approach.

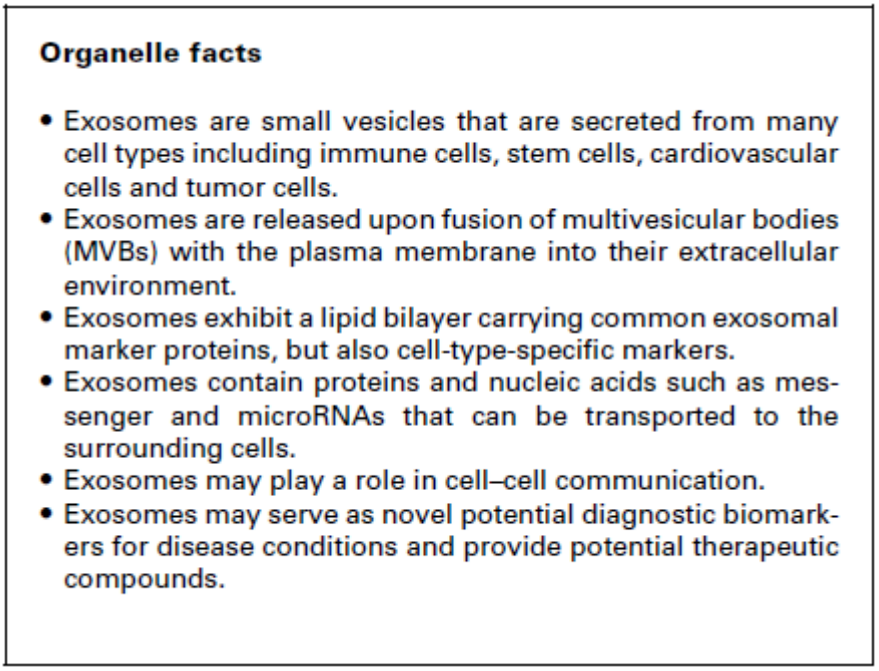

Figure 1.3 General features of exosomes. From Bang and Thum, 2012.

1.2.1 EXOSOME GENERAL FEATURES, CONTENT AND FUNCTION

Exosomes represent a class of cell-derived nanovesicles that originate from the endosomal pathway and are released through different mechanisms from cells to the extracellular space in several biological fluids [39,42,46–49]. Their size ranges between 30 and 150 nm diameter and from a molecular point of view they are known to express specific protein markers such as CD63, CD9, CD81, Alix, TSG101 and hsp70 [39,42,46–49] (Table 1.4).

The exosomal content, which only in part reflects the producing cell, includes mRNAs, microRNAs, DNA and proteins (Figure 1.6). This knowledge is the key to their function and importance, as they could be considered important players in intercellular communication, both locally and systemically. This should be attributed to the fact that, due to their biogenesis, exosomes are composed of a lipid bilayer which makes extremely easy for the particles to be internalized by target cells, as the composition is virtually the same of the cell membranes [39,42,46–49].

Their content, as well as their surface protein expression, renders these nanoparticles very interesting in the diagnostic field and in the search for innovative clinical biomarkers [50].

Regarding their mechanism of action, exosomes are considered to be secreted from most cellular types and to be received by most cells, thus inducing genotypic and phenotypic changes in the recipient cell. For this reason, in the specific tumor environment exosomes are known to be profoundly involved in the delivery of pro-tumorigenic, pro-invasion and pro-metastasis messages to the neighbor cells [51,52].

Table 1 – Attributes of extracellular membranous microvesicles.

	Exosomes
Size (diameter)	30–100 nm
Flotation density (rate zonal centrifugation)	1.10–1.21 g/mL
Morphology	Cup-shaped
Lipid composition	LBPA, low phosphatidylserine exposure, cholesterol, ceramide, contains lipid rafts, sphingomyelin
Protein markers	Alix, TSG101, HSC70, CD63, CD81, CD9
Site of origin	MVBs
Mode of extracellular release	Constitutive and regulated
Mechanism of discharge	Exocytosis of MVBs
Composition	Proteins, miRNA, mRNA

Figure 1.4 Attributes of Exosomes. From Mathivanan and Simpson, 2010

BIOGENESIS

Conversely to shedding microvescicles, exosomes are known to derive from the multivesicular bodies, which are a specialized subset of endosomes [43] (Figure 1.4). These vesicles are integrated in the endocytic system and, once the multivesicular bodies fuse with the plasma membrane, exosomes are released in the extracellular space. The formation of these nanovesicles could occur in two different ways: the first mechanism depends on the Endosomal Sorting Complex Responsible for Transport (ESCRT), while the second one is independent from this complex [43] (Figure 1.5). It is not excluded that the exosomes' production could vary depending on the cell type and the exosomal content. Still, the biogenesis of exosomes is a complex and elusive mechanism, which requires further investigations [43].

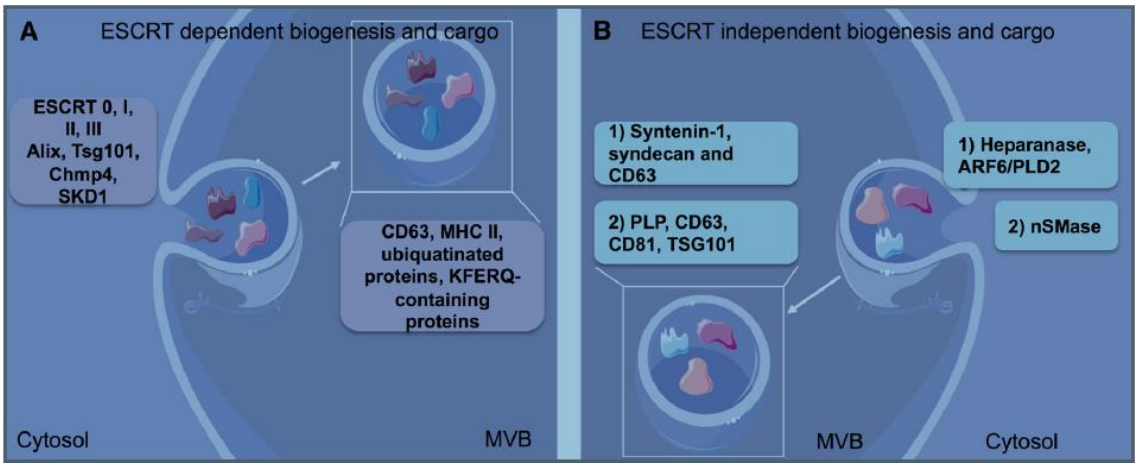

Figure 1.5 Molecular mechanisms of ESCRT-dependent (A) and –independent (B) exosomes' biogenesis. From Abels and Breakefield, 2016.

COMPOSITION

Many approaches have been adopted in order to analyse exosomes' protein content, such as: i. mass spectrometry (MS), western blotting, fluorescence-activated cell sorting (FACS) and immuno-electron microscopy [53]. The exosomal content varies because of many factors, such as the cell type, differentiation stage and specific features of the cell of origin [48,54].

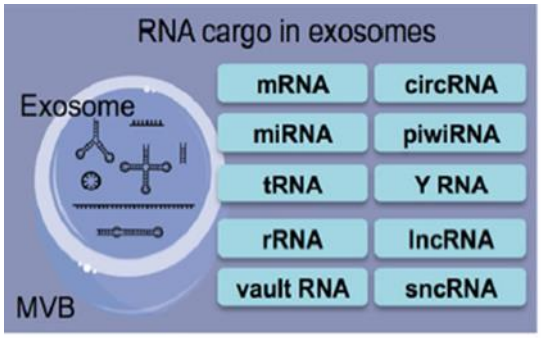

Figure 1.6 RNA species found in EVs. From Abels and Breakefield, 2016.

Even though their composition might change, some proteins were detected as constant in exosomes, no matter the origin [43,46,55]. Some of these proteins are tetraspanins (CD63, CD81 and CD9), proteins involved in the membrane trafficking and fusion (Rabs family and several annexins), ribosomal proteins, metabolic enzymes, heat-shock proteins (HSP60, HSP70, HSPA5, CCT2 and HSP90), Alix, clathrin and TSG101 (Figure 1.7).

Moreover, there are some other proteins that could be considered cell-specific and can be used to recognize cell-specific exosomes (e.g. CD61 for platelet-derived exosomes) [43,46,55].

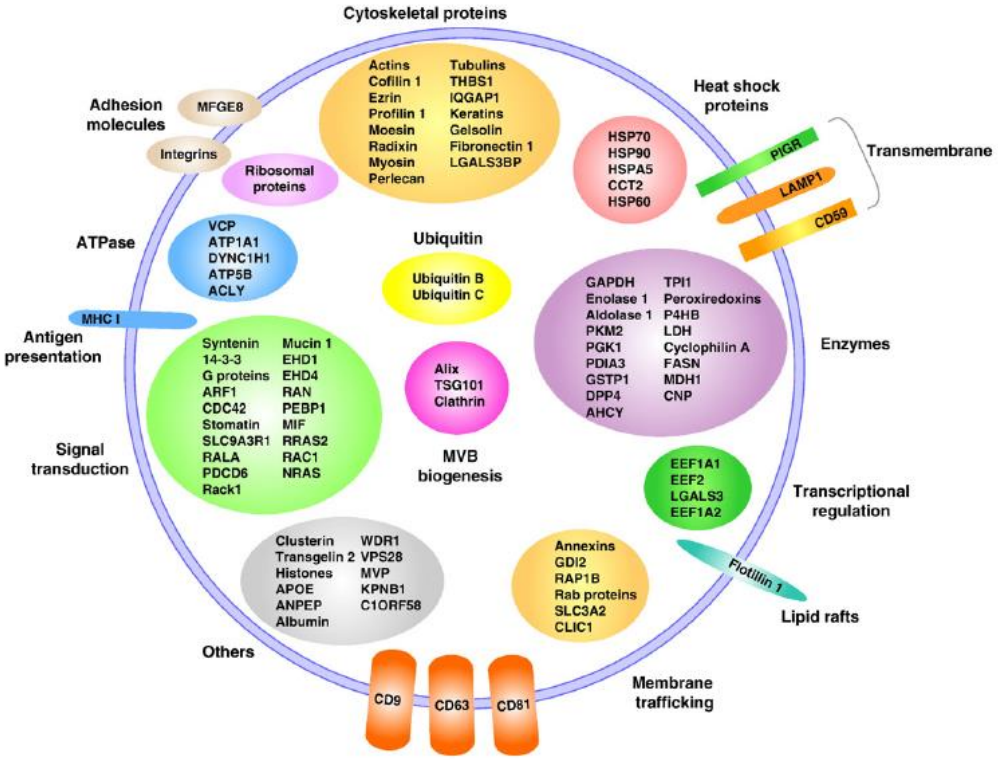

Figure 1.7 A graphical representation of the protein composition of exosomes categorized as per function performed. From Mathivanan and Simpson, 2010

INTERNALIZATION

The exosome-mediated intercellular transfer of both proteins and nucleic acids has, nowadays, attracted considerable attention as exosomes may promote the development of cancer and other pathological conditions [51,56]. Although the functional effects of exosomes mostly rely on the internalization and the subsequent release of contents in recipient cells, the elucidation of their uptake mechanisms and how these may be targeted remains an important challenge [57]. The understanding of these mechanisms can be used to use/develop exosomes as therapeutic agents. In fact, unlike nanoparticles synthesized *in vitro*, exosomes that are released from host cells are not cytotoxic and can transfer information to specific cells, based on their composition and the substance in/on

the exosome [58]. The putative mechanisms of internalization of EVs are summarized in Figure 1.8.

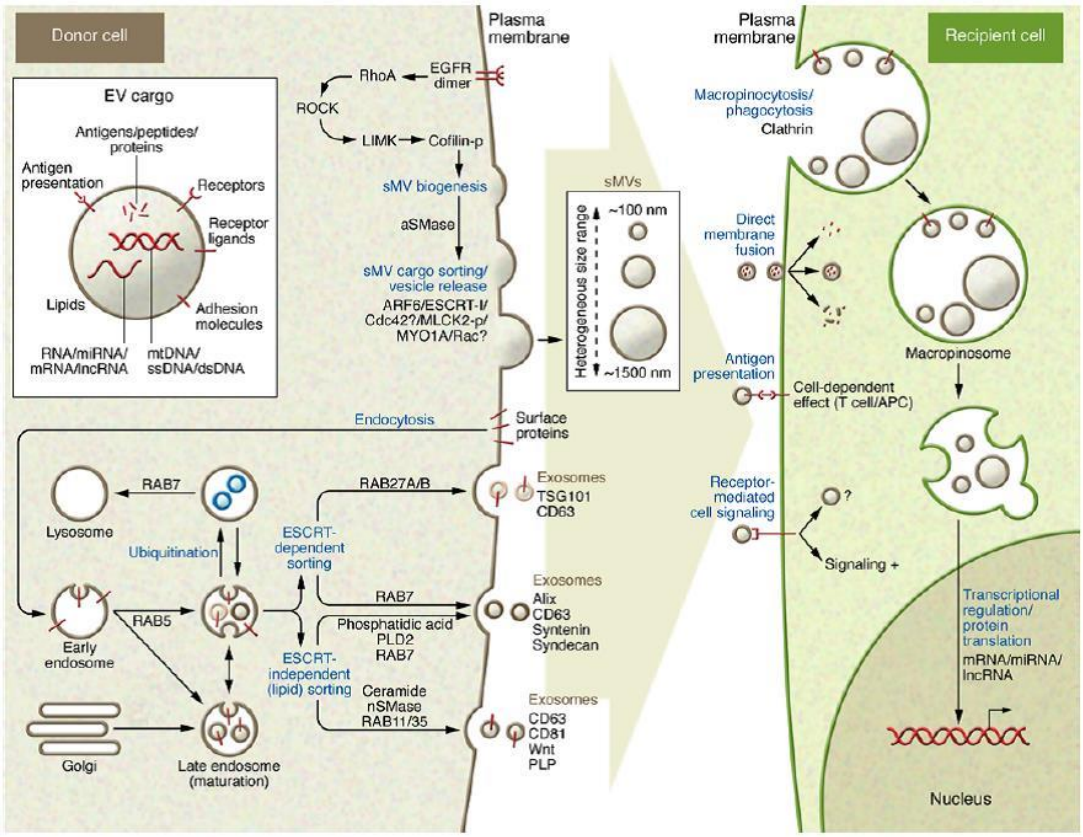

Figure 1.8 Proposed molecular machineries involved in EV (exosome/sMVs) secretion and recipient cell uptake. From Xu et al. 2016

Therefore, drug delivery by exosomes could be a novel mean to transport small molecule drugs to specifically target tissues or cells in a non-cytotoxic manner. Recent evidences indicate that an exosomal drug delivery system is feasible, safe, and may be efficacious against multiple diseases in the future[56-58]. Nanoparticles escape the vasculature through leaky endothelial tissue by the Enhanced Permeability and Retention effect (EPR effect), a process known as "passive targeting" [47]. This is a size-specific property of nanoparticles circulating in the blood stream. Particles must possess a specific size in order not to be entrapped in the *interstitium*, thus flow through blood[45]. Depending on the experimental system used, particles of ~20–100 nm in diameter are very efficiently delivered to target tissues. As comparing sizes of exosomes released from different types of cells, it is considered that certain types of cells may release extracellular vescicles of a smaller than

20–30-nm size range, altering the size of exosomes may be a way to affect tissue targeting and enhance biological responses [58].

FUNCTION

As the knowledge on these particles increased, the more attraction exosomes gained. Numerous functions have been hypothesised for the role of these particles in many biological processes [39,46,47,52]. In immunology, for instance, exosomes carry antigens that are processed by antigen presenting cells and presented to T cells, thus influencing adaptive immunity, but can also carry molecules that promote innate immune responses [61]. Moreover, evidences, from our laboratory among many others, report that exosomes are able to affect tumoral progression[37].

One of the main features of exosomes that makes them so interesting is their function as shuttles in cell-cell communication [62,63]. These nanovesicles, in fact, are very efficient in delivering messages from the producing to the recipient cell under the form of DNA, RNAs and proteins. This exchange of genetic material is fundamental as it could induce modification in the expression pattern, protein content and function of the recipient cell, thus influencing its physiopathology [39,64] (Figure 1.9).

This concept is the most attractive feature of exosomes, as they could be used as biologically active vectors that could send specific signals from one cell to another tumor cells'. Exosomes, for example could contain specific RNA that activate, in target cells, pathways that promote tumour progression [39,64] (Figure 1.9).

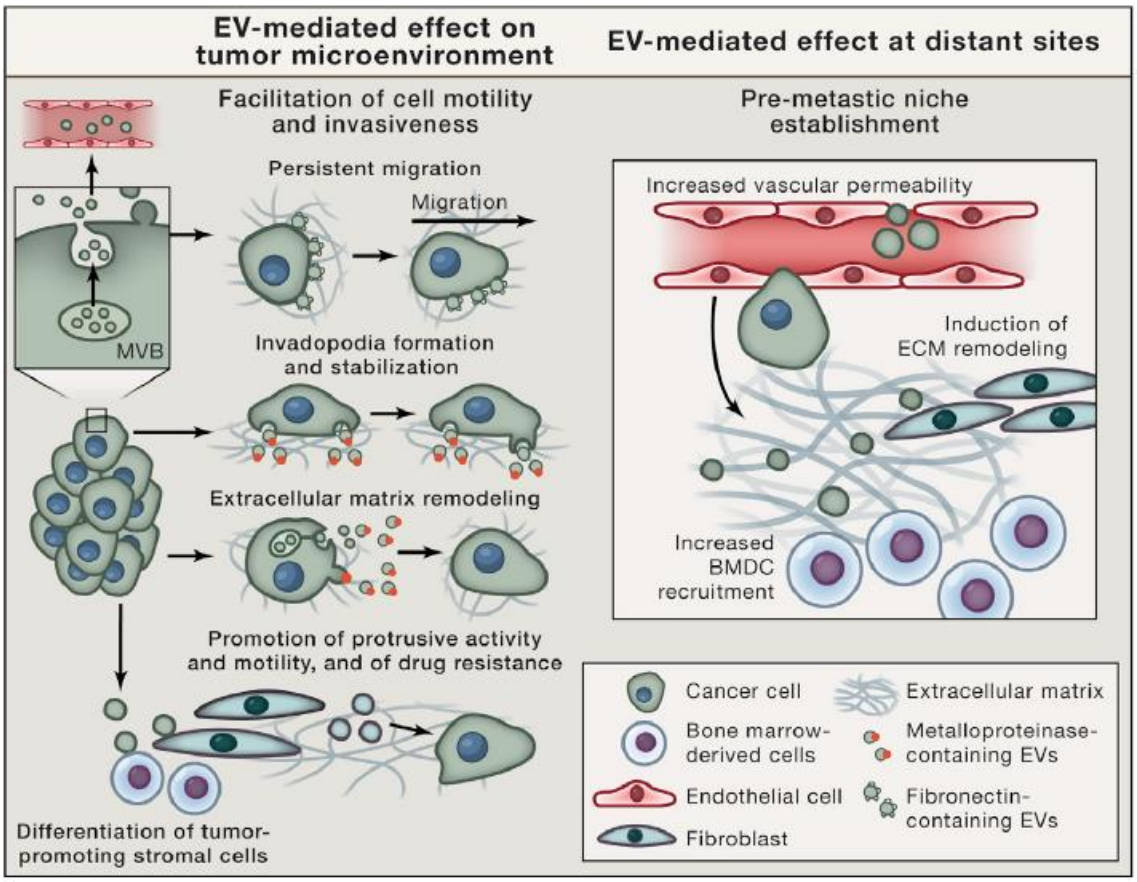

Figure 1.9 EV-mediated effects promoting tumor growth, invasiveness, and metastasis. From Tkach and Thery, 2016.

This concept opens a new interesting field for diagnostic studies based on the analysis of exosomes, in particular their content, as a way to detect the "signature" of a physiological or pathological state [65]. As they are easily accessible (they can be obtained from many biological fluids such as saliva, urine, blood, ascites, etc.), the analysis of the exosomes contained in the biological fluids could be used as new diagnostic and prognostic markers and can allow obtaining information on the diseased tissue without requiring a biopsy [65].

Moreover, the use of exosomes could also be therapeutic in many different conditions, such as cancer or immune diseases. Regarding cancer, although in many articles exosomes are identified as tumor promoters [51,67], it is still not excluded that exosomes could have some kind of anti-tumoral properties [68]. Nonetheless, the prevalent idea is to "engineered" exosomes with oncosuppressive signals to be used in the patient [56,66]. This

new approach is named "EXOcure" [66]. So far, many trials have started, especially in degenerative syndromes and cancer, although much is still left to further investigation[66-68].

EXOSOMES AND GLIOMAS

As previously mentioned, in 2008 Skog et al. reported that glioblastomas secrete a population of nanovesicles that promote tumor progression through the delivery of genetic material, such as RNA, and proteins, and that these vesicles could be used as tools for diagnostics [40].

Al-Nedawi et al. as well as Li et al. reported the undeniable activity of exosomes as carriers of the oncogenic protein EGFRvIII and coding/non-coding RNAs, respectively, in gliomas [69,70].

Still, the mechanisms underlying the influence of exosomes in GBM progression and its communication with the tumor microenvironment is still to be understood. Furthermore, glioma-derived exosomes have been considered as key players in the tumor microenvironment activation and in the mechanisms of increased proliferation, angiogenesis, invasion, clonogenicity, and immune-resistance [74,75].

Nowadays, researchers are spending huge efforts on different sides, trying to exploit the potential of exosomes either as putative biomarkers, as immune-tolerant vectors and targets to interfere with for the tumour-microenvironment communication, [47,64].

1.2.2 THE ELUSIVE NATURE OF EXOSOMES: ISSUES ON EXTRACTION AND QUANTIFICATION METHODS

Considering the enormous clinical potential of these particles, it is fundamental to develop methods that allow obtaining highly purified preparations of homogenous and functionally competent nanoparticles, devoid of contaminants and precisely quantified [50,77]. This would be important also for biodistribution studies or just for mere molecular characterization of these nanovesicles.

Literature on the methods to isolate and purify EVs is extremely vast, but still no gold standard has been totally approved among the scientific community and comparative studies are rare [50,53,54,59,76,77].

Another important issue is the lack of methods to assess the actual purity of the EV preparations. The latter is pivotal especially for functional studies, such as uptake studies, cell-cell communication and activation [78].

Finally, quantifying exosomes is a mandatory step necessary for therapeutic applications [50,82]. There are various methods, some optical and some non-optical, that have been developed to measure or quantify the particles [79–81]. These measurements are usually strictly based on one feature of the vesicles, such as size, scattering properties or molecular features (total protein content or exosome-specific protein content of the EV preparation). Still, no method is able to exactly represent the whole EV population but the research is moving in that direction, confirming the bounty of the potential of extracellular vesicles as well as their relevance in the clinical context [79–81].

1.2.2.1 EXOSOME ISOLATION METHODS

The isolation of extracellular vesicles, and specifically of exosomes, could be obtained through different techniques (Figure 1.10). These methods include differential centrifugation, filtration, polymer and immuno-precipitation and microfluidics [59,76,82,83]. The oldest procedure was ultrafiltration, followed by ultracentrifugation that has been improved for the study of viruses by Svedberg in the 1920s. Later, immunoaffinity purification has been used as a technique for their isolation. These methods, appropriately developed, have been applied for the isolation of extracellular vesicles and even if nowadays a gold standard has not been commonly approved for exosomes isolation, it is believed that a combination of these methods could reach the desired levels of concentration yield and purity [59,83]. Over 60% of authors performing researches on extracellular vesicles are known to use a combination of methods, among which size exclusion chromatography, filtration and density gradient centrifugation are the most used [59,83].

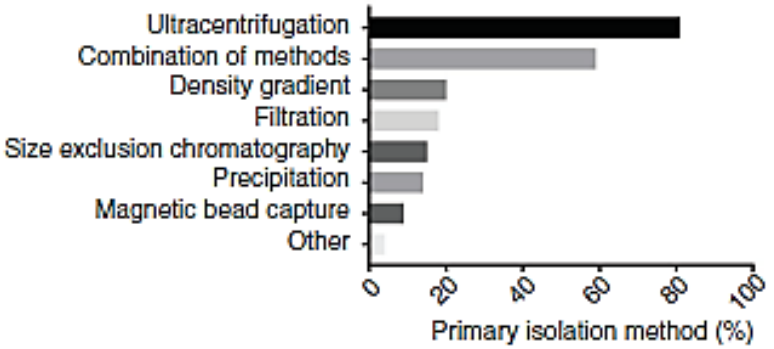

Figure 1.10 Primary exosomes' isolation methods reported in literature. From Gardiner et al., 2016.

CENTRIFUGATION

As shown in Figure 1.10, centrifugation methods have always been the most used to purify exosomes. In fact, this technique is applied in 80% of all exosomes purifications [59,83].

The protocol of isolation involves an initial centrifugation at low speed to eliminate bigger particles, followed by high-speed centrifugations (100,000-120,000x g) in which extracellular vesicles are pelleted [84].

Much attention is needed in the setting of the parameters of the ultracentrifuge, such as rotor (fixed angle, swinging bucket), viscosity of the sample and speed specifics. Obviously, there could be a discrimination of particles based on their size, as the more dense/heavier particles could be precipitated easier than the lighter and less dense ones [84]. The density indeed could be due to the amount of the exosome cargo. Moreover, the "weight" of the particles could influence their precipitation, meaning that heavier particles are more likely to precipitate earlier rather than lighter particles, which might need longer time or higher speed, thus selecting specific subpopulations of EVs [84]. A possible occurrence might be the aggregation of EVs with contaminants or with each other, and for this purpose, resuspension in phosphate buffer solution (PBS) and subsequent centrifugation might be needed to remove further impurities, despite the possibility of diminishing the yield [84].

An implementation of the initial protocol, in order to obtain a purer sample of EVs is to add a density gradient step. Density gradient centrifugation enables us to locate EVs in a floating sucrose gradient efficiently separating protein aggregates and contaminants from the EVs [84].

Many authors describe numerous variations of the original protocol, depending on the assays that are needed to be performed (such as functional or molecular) and based on features such as yield or protein, RNA and total exosomes required and levels of purity from contaminants [50,53,59,76,77,85].

SIZE EXCLUSION

One other common method for the enrichment of samples in EVs is either using filters or chromatography [84].

The fist method is achieved using specific size filters in which the particles smaller or larger than a certain number are excluded. The aim is to retain the desired particles in the filter [82–84].

Using the same concept, column chromatography permits the enrichment of a specific EV population by the sequential elution in a single column. Usually, the filters used are 0.8 μm (for removal of large contaminants) and 0.2 μm (for EVs concentration) [50].

Nevertheless, as these vesicles appear to be particularly delicate, it is possible to damage the sample when processed through much smaller or larger pores. Despite this, the method enables not only the enrichment of the sample, but also the concentration of the sample itself. For this reason, these procedures are preferred as combined to other methods, such as ultracentrifugation or polymer precipitation [83,86].

IMMUNOAFFINITY ISOLATION

The technique of immuno-affinity isolation is based on the recognition of specific proteins situated on the surface of the EVs. The protein-antibody bond enables us to select the marker positive EVs or eventually to negatively select the other populations [86].

In this procedure, the matrix is bonded covalently to EVs-specific antibodies that permit the enrichment in EVs through low-speed centrifugations or magnetic affinity

procedures. This method, as the size exclusion one, is usually associated with other techniques. One of the benefits of this method is its high specificity, which is fundamental either in case of purification or in case of enrichment of the sample in a specific population. Conversely, this approach has a relative low yield, and the stringent conditions applied could identify just one population that is positive to the specific marker, depleting the sample of the other EVs subpopulations [50,86].

MICROFLUIDICS

Beside polymeric compounds, also novel microfluidic devices have been developed in order to isolate EVs. One of these methods require a device that using the antibody-EV surface marker is able to isolate EV from sera as well as culture media. Most of these methods are actually used for non-biological nanoparticles and are currently being readapted to isolate biological EVs based on their biological properties, although many progresses still need to be done [86].

POLYMERIC PRECIPITATION

As enrichment of EV has become a high lucrative goal, many commercial kits have been released, among which the most used is Exoquick (System Bioscience), involving the use of polymeric compounds that embody isolation potential [86]. These kits generally require an overnight incubation and a subsequent centrifugation. These methods have been largely used as they require little expertise and work time. Moreover, it has been reported that this technique has the highest recovery in terms of small EVs subpopulations as well as RNA [59,83]. On the other hand, these methods result in a less pure sample, affecting the actual yield of the preparation in terms of quality. In fact it has been demonstrated the presence of non-exosomal contaminants (such as serum or medium proteins) that co-precipitate with the actual EVs. For this reason, it is important to assess the features of the enriched sample depending on the further uses this sample is needed. Another important consideration is the source of EVs, as there are some samples, such as saliva, in which authors describe Exoquick method as the best one to isolate exosomes, despite the impurities present in the preparation [85]

1.2.2.2 EXOSOME QUANTIFICATION METHODS

It is obvious that before investigating the functional or therapeutic ability of the particles, they should be biophysically characterized [50]. Their particular small size is at the same time their strength (from a functional point of view) and our weakness as exosomes can be below the sensitivity level of many characterization and quantifying methods. Nowadays, novel methods for detection and quantification are being developed and assessed. It is important to acknowledge that, as for the isolation methods, there is not a certifiable gold standard for the detection and quantification of particles [83,86].

As mentioned previously, quantitative and qualitative methods of detection of EVs could be distinguished in optical and non-optical and it is accepted that each method need further optimization and standardization [83,86]. At the 2012 International Society of Extracellular Vesicles (ISEV) workshop in New York City, among various topics, the methods for detection of EVs have been thoroughly discussed, and the most used are represented in Figure 1.11 [83,86].

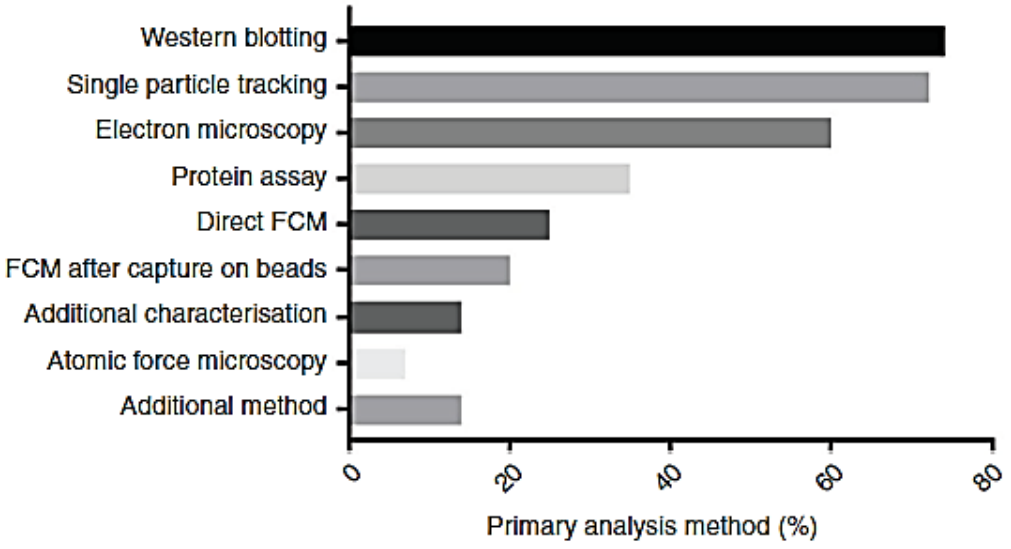

Figure 1.11 Methods used for EV characterization reported in literature. From Gardiner et al. 2016

On this subject, Van der Pol et al. was able to provide measurements of exosomes using different optical and non-optical methods and compare them with that measured by transmission electron microscopy (TEM), which was considered as the gold standard

[83,86]. In the following discussion on this challenging issue, we will review the most common methods, reporting, when possible, comparative studies [79–81].

ELECTRON MICROSCOPY TECHNIQUES

The gold standard among the optical methods for detection of EVs is Electron Microscopy (EM). The protocol implies, with or without paraformaldehyde fixation, the staining of the particles with heavy metals (uranyl-acetate or osmium tetroxide) in order to contrast the vesicles [81,83,86]. This method is extremely useful to characterize the size and the morphology of exosomes [83,86]. Another technique is the immunogold-TEM, in which surface markers are bonded to gold nanoparticles that precipitate and therefore are detectable through transmission electron microscopy. Other techniques include cryo-EM and SEM (scanning electron microscopy) [83,86]. Though extremely useful, these techniques have the flaw that are not quantitative and not only requires specialized materials and expertise, but they is also time consuming and susceptible to the already fragile preparation [86].

ATOMIC FORCE MICROSCOPY

Atomic force microscopy (AFM) has been recently considered as a very powerful instrument for the detection and characterization of nanovesicles and for this reason many publications on EVs report the use of this approach. This method does not require sample preparation, and offers a three-dimensional image of the preparation. Moreover, AFM gives information about the structure, the mechanical and biophysical properties of the sample and, if tip has been functionalized, gives a molecular readout of the EVs detected [86]. Experimentally, AFM is based on a cantilever, appropriately set in terms of deflection and elastic module, which scans a surface, and reveals its topography. For this reason, AFM (compared with TEM in Figure 1.12) is particularly indicated in the detection of nanoparticles, as the resolution of the instrument is infinitively high. This permits also an accurate representation of the EVs morphology [86]. One the other side, as for electron microscopy, the technique requires very expensive instruments, is time-consuming and gives a non-quantitative result [86].

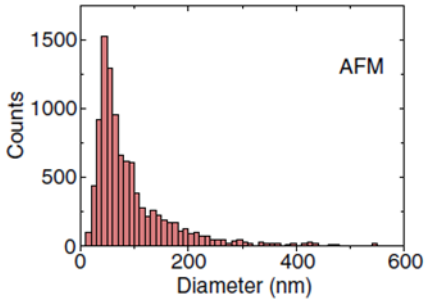

Figure 1.12 Representation of size distribution comparison between TEM (red) and AFM (black).From Van der Pol et al., 2014

OPTICAL SINGLE PARTICLE TRACKING

An optical method to examine nanoparticles in a preparation is using specific programs that take advantage of nanoparticles features [86]. With this purpose, Nanoparticle Tracking Analysis program (NTA) and Nanosight (the instrument) (compared with TEM in Figure 1.13) have been introduced not only for the detection of metal nanoparticles, as it were, but also for biological nanoparticles, such as exosomes [79,81].

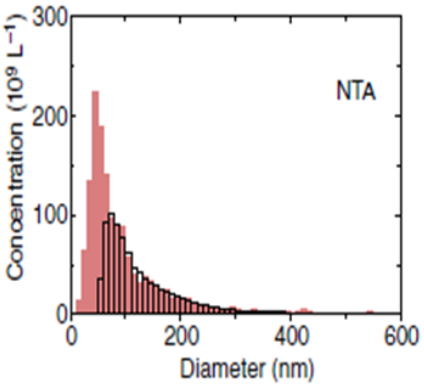

Figure 1.13 Representation of size distribution comparison between TEM (red) and NTA (black). From Van der Pol et al., 2014

This method is constituted of a laser beam that scatters through the particle solution and based on their Brownian motion, through specific equations and algorithms, the program gives a read-out in terms of size distribution and concentration [79,81]. NTA is reported as a very useful method to detect size, concentration and distributions of

particles, but the polydispersity of the sample could be an important deterrent in the estimation of the exact size of the particles. For that, very careful setting of the optimal parameters is required especially when we face heterogeneous populations of EVs. Obviously, these weaknesses are almost non-perceptible when we face a monodisperse solution such as a one-metal or two-metal particle solution, also because their scattering intensity is higher [79,81]. Nevertheless, when we face a polydisperse, biological (thus less scattering) solution, the quantification could be challenging. A new frontier that is currently being exploited is the use of fluorescent NTA programs that are not only able to track the particles, but to recognize the fluorescently labeled ones (for example by antibodies recognizing specific surface markers) as the actual population we want to characterize [79,81]. In fact, NTA is not able to establish if the particles that are detected are effectively the population we want to assess. For this reason, NTA is extremely useful once the method of isolation (especially for samples with huge amounts of contaminants, such as blood or saliva) is standardized and is optimized for the selective isolation of a specific EVs subpopulation [86].

RESISTIVE PULSE SENSING

Another novel instrument, commercialized for the detection of the size distribution and concentration of EVs, is named IZON qNano, which uses the resistive pulse sensing principle [86]. This approach is based on the detection of single EVs that are transported through nanopores in a membrane (or different membranes, based on the heterogeneity of the preparation) by an ionic current. As the biological particles' suspensions are polydisperse, this method, as well as NTA, requires different corrections and care in the setting of the correct protocols for detection of the whole EVs population [79,81].

DYNAMIC LIGHT SCATTERING

With a functioning principle similar to NTA, dynamic ligıı scattering (DLS), compared with TEM in Figure 1.14, is able to detect the size distribution of an EVs preparation [86]. Its major weak point is the fact that this method is particularly sensitive to

polydispersity, thus this method, although it could be improved with advanced software, is not particularly recommended for EVs analysis [81].

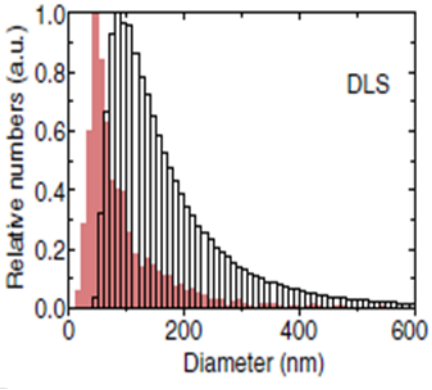

Figura 1.14 Representation of size distribution comparison between TEM (red) and DLS (black). From Van der Pol et al., 2014

FLOW CYTOMETRY

Another method to characterize and detect nanovesicles is flow cytometry (compared with TEM in Figure 1.15) [50,86]. The conventional ones are able to detect only large particles, such as cells and big EVs and the newer the instrument, the more sensitive it is to smaller particles [83,87]. Some of these flow cytometer include Gallios (Beckman Coulter), BD-Influx (Becton Dickinson) and Apogee (Apogee Flow Systems). The protocol implies the use of polystyrene beads with different refractive indexes, which attach to the nanoparticles, making them detectable using light scatter-based flow cytometry [86]. As controls, latex beads could be used in order to set the detection threshold and the right dilution. Many articles have been reported on the use of flow cytometry to detect EVs [86]. The biggest concern with the use of this method is the actual non-detection of the particles per se, but the detection of the beads attached to it [86].

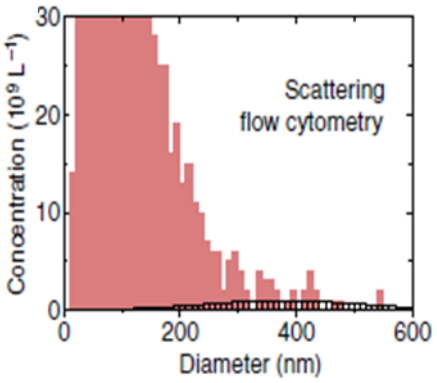

Figura 1.15 Representation of size distribution comparison between TEM (red) and scattering flow cytometry (black). From Van der Pol et al., 2014

On the other hand, the method avoids the detection of protein aggregates or cell membrane debris. Needless to say, the technique is very sensitive and could be a useful tool for EVs detection; still the method needs very careful attention in setting the protocols [87].

WESTERN BLOT

Western blot assay is commonly used to detect EV-common proteins or to identify specific EVs subgroups [50]. This technique is actually the gold standard to molecularly detect EVs. As previously described, the usual markers detected are tetraspanins (CD9, CD63, CD81, CD82), MHC molecules, or milk-fat globule-EGF-Factor VIII (MFGE8, or lactadherin), and cytosolic proteins such as certain stress proteins, Tsg101, Alix, or cytoskeletal proteins (e.g. actin, tubulin) [46]. After EVs purification (either methods are compatible), the protocol is consistent with the one of a conventional western blot. The endpoint is the visualizing of the proteins by SDS-PAGE. Even if this technique is quite sensitive and is able to identify different populations of EVs based on their positivity to specific surface markers, the greatest weakness is the inability of this technique to discriminate the origin of the proteins detected (proteins are also present in cells or other EV, for examples), thus it is very sensitive to the isolation method and the purity of the preparations [86]. Still, the minimal criteria for isolation, detection and quantification of EVs, are yet to be standardize.

2 AIM OF THE STUDY

EVs, and especially exosomes, have been widely recognized as particles able to functionally modified receiving cells upon their uptake. For this reason, in the understanding of the communication between the tumor microenvironment and the tumor cells, exosomes peaked up as putative key players in this dangerous cross talk.
For example, our laboratory has been able to isolate mesenchymal stem cells from the tumor microenvironment of human glioblastomas and we demonstrated that these Glioma Associated Stem Cells (GASC), were able to increase the biological aggressiveness of glioblastoma cells through the release of exosomes.

Recently, many scientists are focusing on the possibility to take advantage of this naturally occurring exosomes-based cell-cell communication system to optimize novel therapeutic delivery systems. This approach, named "Exocure", requires the preparation of highly purified and homogeneous exosomes preparations, functionally competent and correctly quantified.

However, nanoparticles *per se* and especially the biological ones have always been extremely challenging in terms of purification, quantification and assessment.
For this reason, the aim of this thesis was to characterize the exosomal population purified both from a commercial glioblastoma cell line (A172) and from a primary glioblastoma GASC cell line, comparing two different methods of isolation, ultracentrifugation (UC) and ExoQuick precipitation (EQ). Once we proceeded with the purification of the exosomes, we thoroughly characterized the populations obtained in terms of size distribution and frequency, by using Atomic Force Microscopy (AFM) and Nanoparticle Tracking Analysis (NTA), and protein content, by using BCA/Bradford assay and CD9 protein ELISA test. Once characterized the exosomes preparations, we compared their function evaluating, by both confocal microscopy and flow cytometry, their uptake kinetic by A172 glioblastoma cell line. Finally, A172 cells conditioned by the different exosomal preparations were evaluated in terms of motility changes.

3 MATERIALS AND METHODS

3.1 CELL CULTURE

3.1.1 Primary and commercial cell lines

A172 human glioblastoma cell line was grown in Dulbecco's Modified Eagle's Medium (Sigma-Aldrich, St. Louis, MO, USA), supplemented with 10% fetal bovine serum (FBS) and 1% Penicillin-Streptomycin (Euroclone). Cells were maintained in monolayer culture at 37°C under a humidified atmosphere containing 5% CO_2.

Human glioma samples were collected by the Neurosurgery Department of the Azienda Sanitaria Universitaria Integrata of Udine, after a written informed consent was obtained, in accordance with the Declaration of Helsinki, and with approval by the Independent Ethics Committee of the University-Hospital of Udine. Cells representative of the glioblastoma microenvironment, namely the glioma associated stem cells (GASC), were isolated and cultured as in [37]. Briefly, glioma samples were first disaggregated mechanically with scalpels and then enzymatically dissociated in a 0.025% Collagenase type II solution (Worthington) in Joklik modified Eagle's Medium (Sigma-Aldrich) for 5 minutes at 37°C. Collagenase activity was blocked adding a 0.1% BSA (Sigma-Aldrich) solution in Joklik modified Eagle's Medium (Sigma-Aldrich). Cell suspensions were centrifuged at 500g for 10 minutes and filtered through a sieve (BD Falcon) in order to select a population less than 40μm in diameter.

2.0 x 10^6 freshly isolated human cells were plated onto 100 mm human fibronectin (Sigma-Aldrich) coated dishes (BD Falcon) in an expansion medium (MASC) composed as follows: 60% low glucose DMEM (Invitrogen), 40% MCDB-201, 1mg/mL linoleic acid-BSA, 10^{-9} M dexamethasone, 10^{-4} M ascorbic acid-2 phosphate, 1X insulin-transferrin-sodium selenite (all from Sigma-Aldrich), 2% fetal bovine serum (StemCell Technologies), 10ng/ml human or murine PDGF-BB, 10ng/ml human or murine EGF (both from Peprotech EC). Medium was replaced with fresh one every 4 days. Once cells reached 70-80% of confluence, they were detached with TrypLE Express (Invitrogen) and re-plated at a density of 1-2 x10^3/cm^2.

3.2 EXOSOME ISOLATION

For exosomes purification, cells were cultured either in MASC medium or DMEM supplemented with FBS deprived of bovine extracellular vesicles by ultracentrifugation (100.000g for 4 hours at 4°C). Briefly, when A172 and GASC cells reached 50-60% cell confluence, media were replaced with fresh ones and, after 4 days, culture supernatants were collected, aliquoted and kept at -20°C. Once needed, aliquots were thawed and split in two for differential processing (i.e. ultracentrifugation and Exoquick precipitation).

3.2.1 Ultracentrifugation

Ultracentrifugation of culture supernatants was performed as described in [84]. Briefly, culture media from A172 and GASC were centrifuged at 3,000g for 30 min and the supernatants filtered by 0.22μm syringe filters (Millipore, USA) to exclude cell debris and remove microvesicles. The resultant supernatants were diluted in PBS and transferred to 26,7ml polycarbonate tubes for ultracentrifugation at 100,000g for 90 min at 4 °C using a Type 70 Ti rotor in a L-80 XP ultracentrifuge (Beckman Coulter, USA). After removing supernatants, the pellets were washed with PBS and re-ultracentrifuged at 100,000g for 60 min at 4 °C. The pellets were finally resuspended in 500μl PBS.

3.2.2 ExoQuick precipitation

ExoQuick-TC was used to process culture supernatants for exosomes purification, according to the manufacturer's protocol (EQ, System Biosciences Inc.; Mountain View, CA). Briefly, culture supernatants were centrifuged (3,000g for 20 minutes at 4°C) in order to eliminate cells and cell debris. Recovered supernatants were then mixed with ExoQuick-TC solution in a 5:1 ratio and incubated for at least 12 hour at 4°C. Mixtures were finally centrifuged (1,500g for 30 minutes at 4°C) to obtain the exosome pellets, which were resuspended in 500μl PBS.

3.3 EXOSOME SIZE ANALYSIS

3.3.1 Atomic force microscopy

Exosomal-preparations, obtained by both ultracentrifugation and ExoQuick, were diluted 1:5 in PBS to prepare a final solution of 30μl of exosomes. Samples were then placed on freshly cleaved 11x11mm mica sheets for 10 min and dried under a stream of nitrogen. AFM imaging was performed at room temperature on a BioScope Catalyst

controlled by a NanoScope V controller (Bruker), combined with an Eclipse TE2000-S inverted optical microscope (Nikon). Images were acquired in Tapping Mode using ScanAsyst Air probes (SCANASYST-AIR k=0.4N/m) (Bruker).

Using Nanoscope 9.0 software (Bruker), topographic height and phase images were recorded at 256x256 pixels with a scan rate of 1,00Hz, a scan size of about 5µm, and a Z range of 3µm. Images were processed and analyzed using Gwyddion 2.37 software (Department of Nanometrology, Czech Metrology Institute).

3.3.2 Nanoparticle Tracking Analysis

Size distribution and particles concentration within samples were analyzed by measuring the rate of Brownian motion, using a NanoSight LM10 system (NanoSight Ltd., Malvern, UK) equipped with a 532nm laser and a particle tracking software. For each sample, appropriately diluted in PBS (100-200 times), a video was captured for 60s each with a detection threshold set at 16 (maximum). Temperature was monitored throughout the measurements. Vesicle size distribution together with concentration esteem of the NTA profiles were obtained from the raw data files given by the program itself.

3.4 EXOSOME QUANTIFICATION

For the detection of the exosomal protein CD9, Europium Time- Resolved Immunofluorescence assay for detection of exosome antigens CD9 (TRIFIcTM Exosome Assay, Cell Guidance Systems) was used. Exosomal pellets were processed according to the manufacturer's instructions. Protein amounts were estimated by reading the optical density on an Infinite 200 PRO Microplate Reader (TECAN Group Ltd., Switzerland) at 615nm and comparing it with the standard curve supplied by the kit. Samples were run 3 times in triplicates.

Total exosome protein contents were quantified by using Bradford and BiCinchoninic Acid Assay (BCA) protein assays.

3.5 EXOSOME UPTAKE

3.5.1 Confocal and epifluorescence imaging

20.000 A172 cells were incubated for 1, 3, 6, 24, 48 and 72 hours in 10% ultracentrifuged FBS - Dulbecco's modified Eagle's medium (uDMEM) added or not with $1*10^9$ exosomes labeled by DiD (Molecular Probes Invitrogen, Carlsbad, CA, http://www.lifetechnologies.com), according to manufacturer's instructions. Briefly, exosome preparations were incubated for 20 min in 1:200 DiD-labeling solution, and then preparations were re-precipitated to eliminate the excess of fluorophore.

To localize exosomes within a cell, nuclei were stained by adding 2mg/ml Hoechst 33342 (Sigma) to cell cultures 15 min before imaging. At each defined time-point, DiD-labelled exosomes were removed and wells carefully washed before imaging. Fluorescence images were collected either by Leica TCS SP8 confocal microscope equipped with a 63x oil-immersion objective (Leica Microsystems, Wetzlar, Germany, http:// leica.com) or by a Leica DMI600B microscope equipped with a 40x dry objective (N.A. 0.6) and processed by a deconvolution software.

3.5.2 Flow cytometry

A172 cell cultures conditioned or not by DiD-labelles exosomes as previously described (3.5.1) were detached from the culture substrates by TrypLE Express solution (Gibco — Life Technologies). Detached cells were washed and resuspended in 200µl of calcium- and magnesium-free Phosphate Buffered Saline (PBS) before performing cytometric analyses.

Flow cytometry was performed on a FACSverse flow cytometer (BD Biosciences) on cells detached from substrates with TrypLE Express solution (Life Technologies), washed and resuspended in 200 µl PBS. After reaching a count of $1x10^4$ cells, the data were gated on the basis of forward and side scattering and the mean fluorescence intensity (MFI) was calculated as the ratio between total DiD fluorescence over the number of cells showing fluorescence for both DiD and Hoechst. For each time point, experiments were performed in triplicate and at least 10.000 cells *per replica* were analyzed. All the analyses were performed by using FlowJo V.10 software.

3.6 FUNCTIONAL ASSAY

In order to evaluate the *in vitro* cell motility of A172 conditioned or not by exosomes precipitated, either by Exoquick or ultracentrifugation, from both A172 and GASC supernatants, a scratch assay was performed. $2*10^4$ cells were seeded onto a 24-well ($33mm^2$ area) plate and when reached high cellular confluence, a scratch was created using a 200µl tip. Phase contrast images of the scratches were acquired every 6 hours, until their complete closing, utilizing either Nikon Eclipse TS100 (Nikon) or Leica DMI6000B. Briefly, the motility (µm/hour) was estimated by measuring, by ImageJ software, the average width of the scratches at different time points.

3.7 STATISTICS

Statistics was performed by either Minitab 17 or Graphpad Prism 5.0 (La Jolla, CA, USA). AFM and NTA size data were fitted with a lognormal probability density function to determine the peak size. Results are presented as mean ± standard deviation (SD). Paired or unpaired t-test, as appropriate, was used to compare continuous variables between two groups. For uptake and scratch assays, repeated measurements one-way ANOVA followed by Bonferroni post-test was used. In the case of the motility assays using decreasing concentrations of exosomes, one-way Anova was followed by a test for linear trend. For size, uptake and migration measurements, unless indicated, a p value less than 0.05 was considered significant.

4 RESULTS

4.1 DIFFERENT PURIFICATION TECHNIQUES AFFECT THE SIZE DISTRIBUTION OF THE EXOSOMIAL PREPARATIONS

Three GASC as well as A172 culture supernatants were split and exosomes were precipitated by two different enrichment methods, specifically ExoQuick (EQ) and ultracentrifuge (UC). Once the exosomal preparations were resuspended, they were adsorbed on mica coverslips and subsequently assessed by AFM to determine the size distribution of the isolated exosomes. Figure 4.1a and 4.1b for GASC and Figure 4.2a and 4.2b for A172 are representative images obtained from EQ- and UC- preparations, respectively. Firstly, data collected assessed the spherical-like morphology of the isolated particles. Secondly, they highlighted that particles isolated through EQ had a smaller size with respect to those obtained by UC (Figure 4.1, Figure 4.2)

This was further confirmed by interleveled size distributions, determined from the maximum height of the particles obtained analyzing at least 10 AFM images for each GASC- (Figure 4.1c) and A172- (Figure 4.2c) sample. In fact, independently form the source, glioma associated stem cells or commercial glioma cell line, exosomes size distribution vary depending on the isolation method, being exosomes enriched by EQ smaller than those obtained by UC. It is important to specify that these are the results obtained using AFM images evaluations.

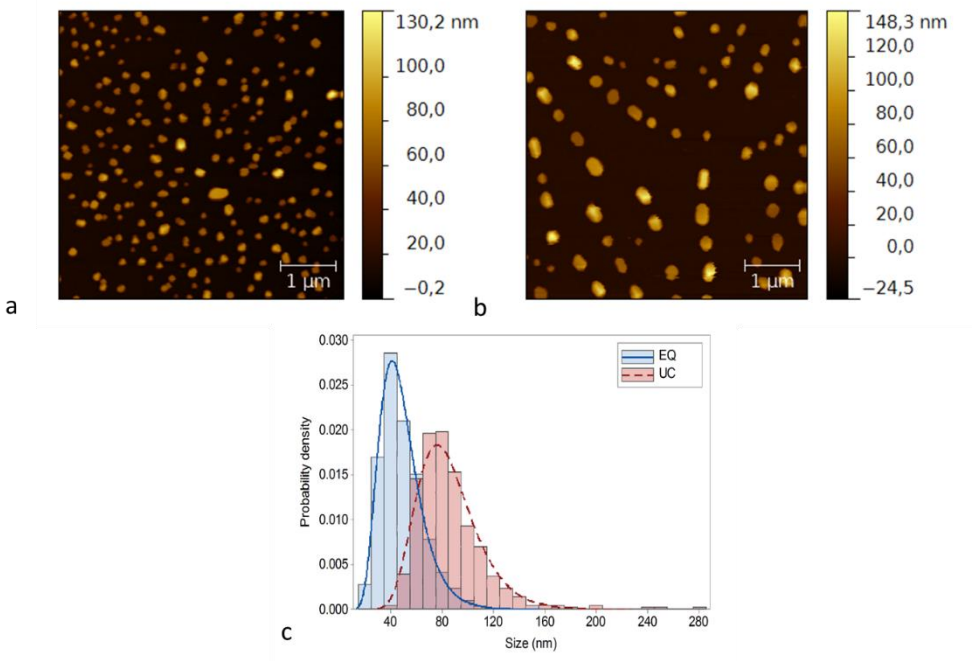

Figure 4.1 Representative image of GASC nanoparticles obtained using EQ (a) and UC (b) precipitation methods. Panel c represents the size frequency distribution of both the preparations, revealing the difference in size of the particles isolated by EQ (n=2140) and UC (n=433), respectively. 5x5µm images. Scale bar: 1µm

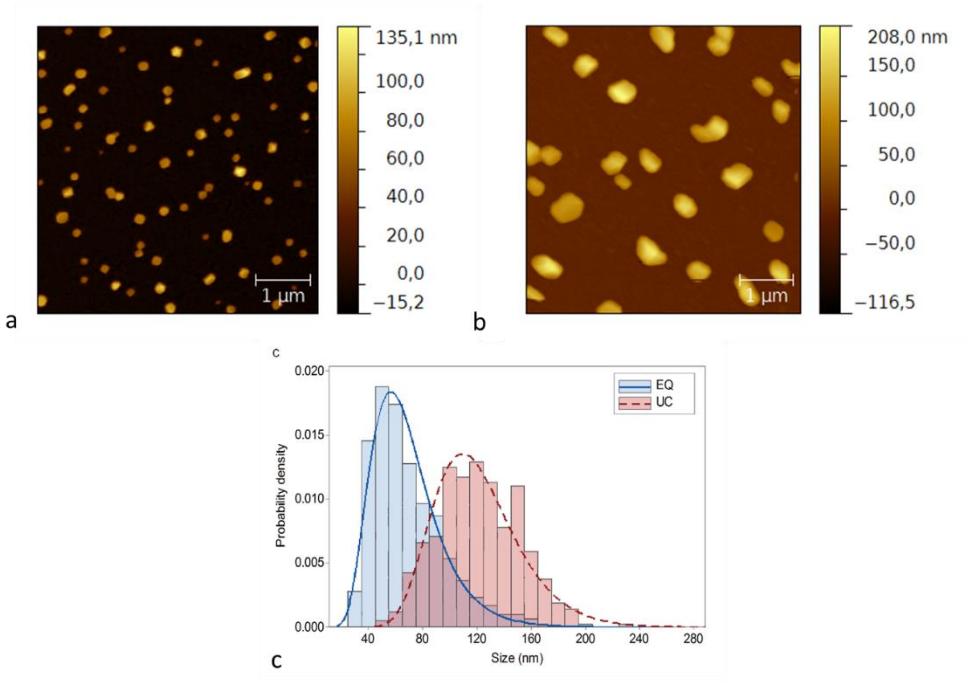

Figure 4.2 Representative image of A172 nanoparticles obtained using EQ (a) and UC (b) precipitation methods. Panel c represents the size frequency distribution of both the preparations, revealing the difference in size of the particles isolated by EQ (n=840) and UC (n=426), respectively. 5x5µm images. Scale bar: 1µm

Three different preparations for each sample and for each method were then statistically evaluated, assessing 10 images for each sample obtained. As reported in Table 4.1, UC

preparations showed larger particles, with an average peak size of 81.1nm and 94.4nm for GASC and A172, respectively. On the other hand, AFM measurements on EQ preparation reported a peak size of 43.3nm for GASC and of 50.8nm for A172. For both A172 and GASC, the differences between EQ- and UC- precipitated exosomes were statistically significant, confirming the divergence of the extracellular vesicles' size based on the isolation approach.

Table 4.1 AFM measurements of GASC and A172 size distributions when isolated by different isolation methods (EQ and UC, respectively). For each exosome source, p values are indicated in the last column.

SIZE (nm)	**EQ**	**UC**	***p***
GASC	43.3 ± 11.7	81.1 ± 3.9	0.0061
A172	50.8 ± 5.7	94.4 ± 13.9	0.0074

The exosomes preparations were furthermore assessed for size distribution using the NTA technology. It was extremely interesting to notice that NTA could not discriminate the difference in the size distribution between the isolation methods

In fact, Figure 4.3a and b represent the interleveled size distributions of the particles isolated from GASC and A172 respectively, using EQ and UC, respectively. The graphs show that for GASC preparations, EQ samples had a peak size of 83.6nm, while those isolate in UC reported a 90.1nm peak size. Moreover, A172 isolated in EQ and UC showed peak sizes at 107.4 and 106.1nm, respectively.

The inability to detect differences between EQ- and UC- preparations, could be probably due to the presence, in EQ preparations, of small particles whose scattering properties could not be detected by the camera of the NTA instrument. Indeed, previous articles reported that NTA is poorly able to detect particles that are below 50nm in diameter (that are instead clearly visible using AFM), thus deeply affecting NTA measurements [79,81].

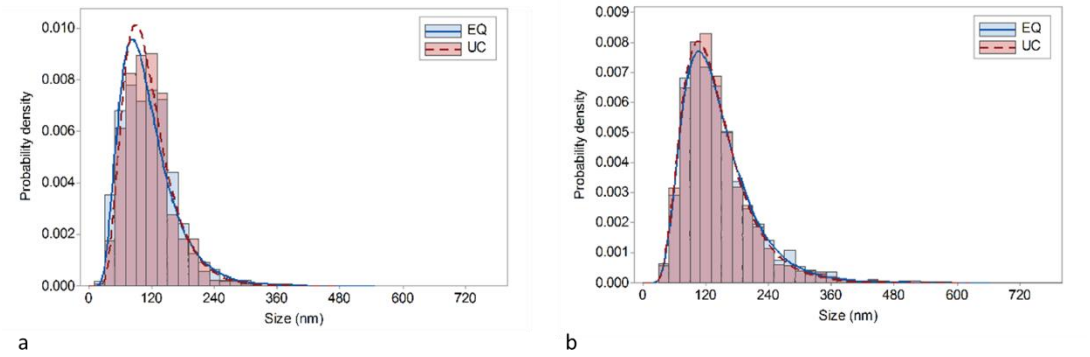

Figure 4.3 Size distribution of GASC (a) and A172 (b) exosome preparations, obtained by both EQ and UC, measured by NTA. For GASC preparations 567 particles for EQ and 654 particles for UC were anaòyzed; on the other hand, for A172 samples, 1838 EQ particles and 1820 UC particles were assessed.

Table 4.2 reports the results obtained when all three sample in triplicate were estimated, confirming the lack of significant difference between samples precipitated by EQ and UC.

Table 4.2 Peak size of GASC- and A172- exosomes, isolated by different isolation methods (EQ and UC, respectively), as assessed by NTA. p values are indicated in the last column for each exosome source.

SIZE (nm)	**EQ**	**UC**	***p***
GASC	78.0 ± 7.1	80.9 ± 10.9	n.s.
A172	92.8 ± 13.8	90.1 ± 10.0	n.s.

Altogether, data obtained suggested that, for UC precipitations both quantification methods seemed interchangeable; nevertheless, in case of EQ preparations, AFM was able to detect a population of particles that was under the range of detection of NTA, supporting the notion that this latter method could underestimate both the actual concentration and the truthful size range of EQ- exosomes. This statement is consistent for both GASC as well as A172 samples. In fact, figure 4.4 compares for EQ- and UC-preparations of A172 and GASC-derived exosomes, the peak size as measured by both AFM and NTA. These graphs show clearly that for UC preparations AFM and NTA measurements are similar (Figure 4.4b), while for EQ preparations (Figure 4.4a), the size shifts based on the quantification method.

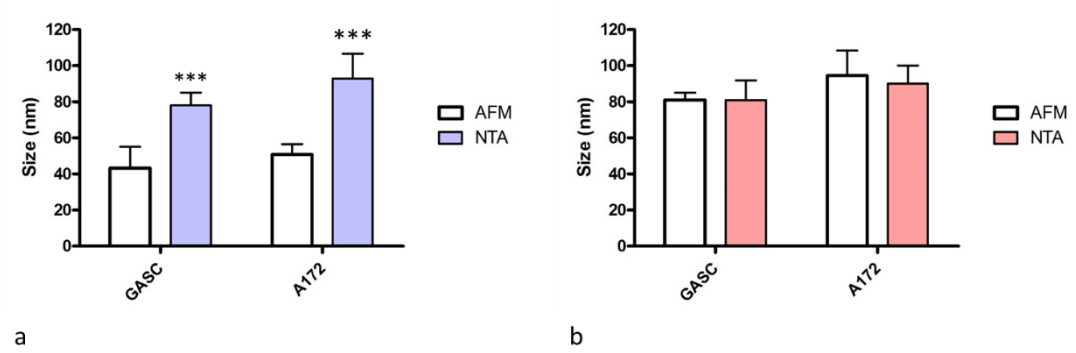

*Figure 4.4 Comparison between the size peak averages obtained from A172 and GASC samples isolated by EQ (a) and UC (b) using AFM and NTA. Data are presented as mean ±standard deviation. p values are indicated as *** if p<0.0001.*

As literature reported DLS as another viable method to quantify nanoparticles [81], we assessed our sample using this approach. The first assays failed, as the instrument is extremely sensitive to the polydispersity of the particle. Figure 4.5 shows an attempt to measure GASC EQ and UC exosomes using DLS and we observed peaks consistent with data obtained by AFM for both samples (EQ and UC showed 41.5 ± 3.2nm and 90.1 ± 0.7nm peaks, respectively). Despite these encouraging results, confirming data obtained by AFM, we also observed peaks at 500nm, probably due to aggregates or debris that compromised the actual measurement because of the intensity contribution of these particles and the evaluation of the polydispersity index of the preparation. In fact, with a polydispersity index of nearly 0.7, the samples often appear not suitable for DLS measurements.

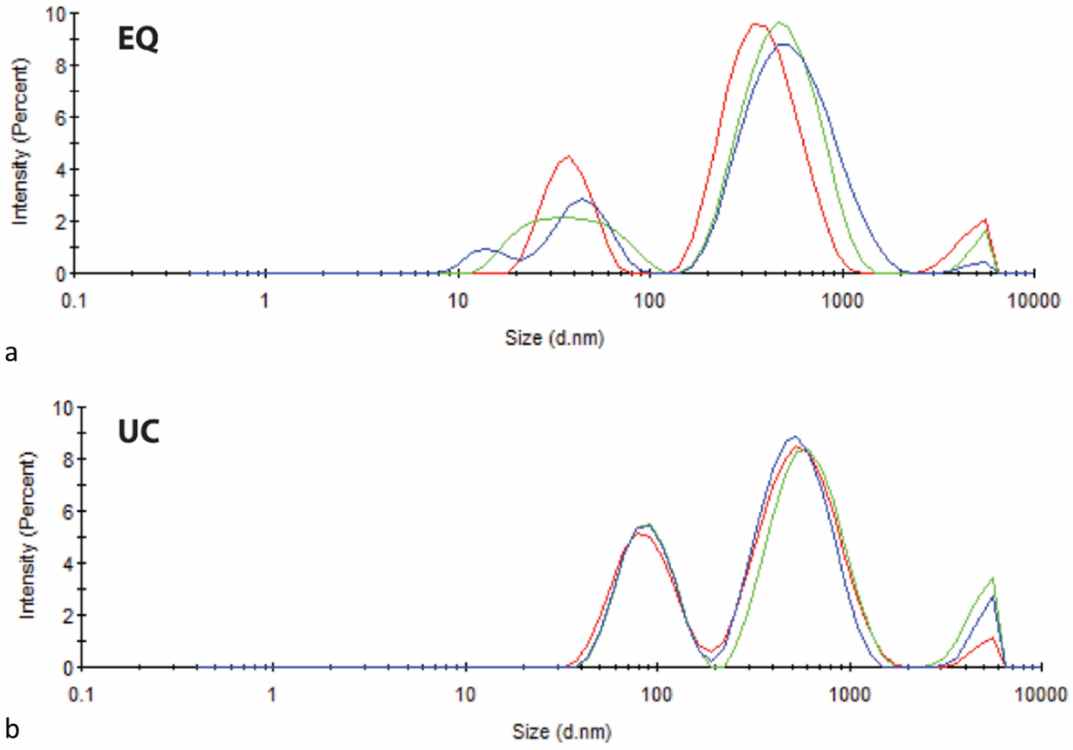

Figure 4.5 DLS plots from GASC-extracted exosomes by EQ (a) and UC (b). The three colors represent the triplicate measurements. In both cases we observe two peaks, the low-scattering exosomes component and the high-scattering debris and aggregates (around 500 nm), respectively.

Another discrepancy revealed using the two different methods of quantification regards concentration. In fact, EQ and UC did not share the same proportion between the amount of particles assessed by NTA and the particle density obtained by AFM (Table 4.3).

In fact, calculating by AFM the particle density (particles/μm^2) for both the UC- and EQ-preparations depicted in Figure 4.1c and 4.2c, and comparing the results obtained counting, as particles/ml, the same preparation using NTA (Figure 4.3a and 4.3b), we observed that EQ samples were characterized, with respect to the UC ones, by a much higher ratio (Table 4.3). As literature reports an NTA threshold limit of detection of 50nm for biological particles due to their scattering properties, we considered applying this cut-off to our AFM data [81]. It is interesting to see that, applying to AFM data a threshold of 50nm, the proportion between the particles measured by AFM and NTA became comparable, both for A172 and GASC (Table 4.3). Thus, the NTA approach for nanoparticle quantification can underestimate the number of particles per volume, if their size is below the detection threshold, and overestimate their average size as well.

In our study, this was especially true when applied to EQ preparations and was consistent for GASC as well as for A172 preparations.

This result is the actual proof that the below-50nm particles were the ones responsible for the discrepancy between AFM and NTA measurements.

Table 4.3 Particle concentration as assessed by AFM and NTA measurements. Particle concentrations are expressed as particles/µm2 for AFM and particles/ml for NTA. The ratio between the two methods reflects the underestimation of NTA for particles that are below 50nm. Further calculations on AFM data, applying a 50nm cut-off reports a corrected particle density and thus a corrected AFM/NTA ratio, that, this time, is comparable between the two methods. This result is especially appreciated in the case of EQ preparations and for the A172 sample.

	Density AFM (particles/µm²)	**Concentration NTA (particles/ml)**	**Ratio AFM/NTA density (a.u.)**	**Density AFM (>50nm) (particles/µm²)**	**Corrected Ratio AFM /NTA density (a.u.) (>50nm)**
GASC EQ	9.23	3.34E+10	2.76E-10	6.86	2.05E-10
GASC UC	2.64	1.68E+10	1.57E-10	2.58	1.54E-10
A172 EQ	5.82	7.80E+10	7.46E-11	3.62	4.64E-11
A172 UC	1.66	3.37E+10	4.93E-11	1.61	4.78E-11

4.2 THE CONTRIBUTION OF THE PURIFICATION TO UC AND EQ PREPARATIONS

The first and most important datum obtained by exosome size analyses was that EQ precipitation gave a size distribution of particles that is smaller than the UC one; moreover, these differences are visible using AFM but are not detected by the NTA technology. Therefore, we tried to assess possible players responsible for the difference in size distribution.

Since EQ-precipitation is based on polymers known to precipitate, together with nanoparticles, also proteins, to exclude the possibility that small-size nanoparticles were indeed an artifact due to the precipitation method, we precipitated culture media and buffer, both by EQ and UC,. Briefly, NTA measurements of the particle concentration in PBS and culture media precipitated by both methods was 4 orders of magnitude smaller than that measured in actual samples (thus almost negligible). Moreover, the size of the particles assessed by either NTA or AFM (>150nm diameter) was compatible with that of big precipitates and not of exosomes (data not shown).

In order to establish if the cut off in size that discriminates UC and EQ could be imputed to the ultracentrifuge inability to precipitate the smallest particles, we decided to re-precipitate an EQ preparation using UC (Figure 4.6). Assessing the particles using AFM we noticed that the EQ preparation that underwent UC precipitation shifted its size peak from 45.3nm to 85.0 nm, compatible with the previous UC observations (Table 4.3). Moreover, not only the size peak was affected by the re-precipitation, but also the particle density measured, which shifted from 3.8 particles/μm^2 (EQ) to 1.1 particles/μm^2 (UC re-precipitation). Therefore, the UC method seemed to be unable to precipitate small particles and therefore the resulting distribution might not be completely representative of the actual exosomal population. This hypothesis was further supported by the comparison between A172 supernatants precipitated by EQ and the preparations obtained by purifying these latter by UC: the smaller particles visible by AFM in the initial EQ preparation disappeared after precipitation by UC, confirming that this latter selects only the larger particles, likely mostly in the NTA range of detection.

All the data considered suggest that the EQ isolation method is able to precipitate a population of the extracellular vescicles that is enriched in small particles and that this population is lost during ultracentrifugation. Therefore, ultracentrifugation might be responsible for a selection of the exosomal population based on size. Moreover, regarding quantification methods, NTA is a technique whose efficiency appears to be isolation method-specific. In fact, despite NTA might be suitable for UC-isolated particles, it might not be the most efficient quantification method when dealing with EQ-extracted exosomes.

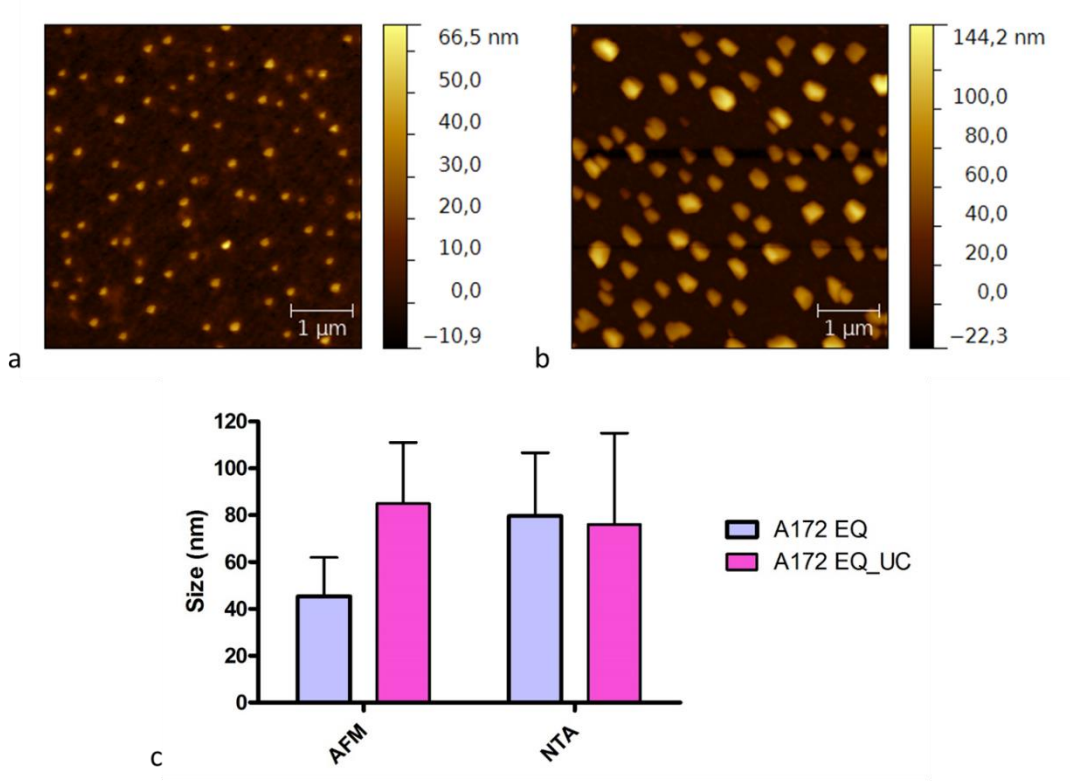

Figure 4.5 AFM representative pictures of A172 exosomes isolated by EQ (a) and subsequently precipitation by UC (b). As observed by AFM measurement (c), EQ isolated exosomes increased in size (result not visible using NTA), probably due to the loss of small particles during the re-precipitation. Data are presented as mean±standard deviation.

Table 4.4 AFM and NTA measurements of EQ isolated A172 exosomes and the same preparation re-precipitated using UC. The size difference between the two precipitations is detected by AFM, but not by NTA. Moreover, the particle density, as well as the particle concentration, changed considerably, demonstrating that UC is able to isolate the bigger particles, failing to precipitate the smallest ones that are included in the EQ precipitation.

SAMPLE	**AFM**		**NTA**	
	SIZE (nm)	**DENSITY (particles/µm²)**	**SIZE (nm)**	**CONCENTRATION (particles/ml)**
A172 EQ	45,31 ± 16,62	3,8	79,67 ± 27,00	4,88*10E11
A172 EQ_UC	85,04 ± 26,04	1,05	76,03 ± 39,05	6,46*10E10

4.3 MOLECULAR ASSAYS ON EQ AND UC EXOSOMES

Methods based on protein determination in the UC and EQ preparations are not reliable for estimating the amount of exosomes in a sample. The data obtained by AFM and NTA quantification methods seem to suggest that EQ isolation method has a higher particle yield compared to UC. We attempted to investigate eventual protein contaminations in EQ as well as UC and eventually evaluate them. We performed Bradford as well and BCA colorimetric assays followed by SDS-PAGE (Figure 4.7). In fact, Bradford, BCA and SDS-PAGE show that EQ precipitation introduces an overwhelming background of proteins, likely due to precipitation of serum proteins from the media. The results obtained are summarized in Table 4.5.

Table 4.5 EQ preparations have a much larger protein content than UC. Protein concentration were measured in triplicate using both Bradford and BCA colorimetric assays on the four samples indicated and the resulting concentration in µg/ml was divided by the particle density measured by NTA (particles/ml) to obtain the amount of protein/billion exosomes. p values are expressed as the significant difference between the isolation methods.

		Protein/billion exosomes (µg) Bradford assay		**Protein/billion exosomes (µg) BCA assay**	
GASC	**EQ**	5.55 ± 0.21	*p<0.0001*	6.16 ± 0.55	*p<0.0001*
	UC	0.68 ± 0.08		1.43 ± 0.09	
A172	**EQ**	27.53 ± 3.23	*p=0.0001*	38.02 ± 1.42	*p<0.0001*
	UC	1.04 ± 0.18		1.68 ± 0.08	

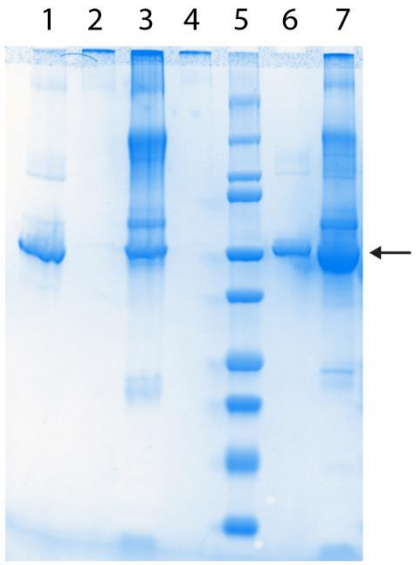

Figure 4.6 SDS-PAGE gel reveals the protein content of 0.5x10^9 exosomes preparations from GASC isolated using EQ (1) and UC (2). Lanes 3 and 4 are the same setting using A172 supernatant (EQ and UC, respectively). Lane 5 shows the Bio-Rad Dual Colour Standard protein marker, whereas lane 6 was loaded with Bovine Serum

Albumin (molecular weight = 66 kDa) and 7 with FBS. The resulting gel reveals a greater protein content in EQ preparations rather than UC preparations.

All of these methods have revealed to be unfit to efficiently quantify the exosomal fraction in both preparations. Therefore, we decided to evaluate the CD9 content of the preparations through a CD9 ELISA assay that combined with NTA, estimates the exosomal content of each sample. CD9 (or CD81 and CD63) detection could be used as a general method for exosome quantification, however exosomes from different sources are likely to present different amounts of these markers. In the case of uptake studies in which exosomes from different sources are compared, this would make the normalization impractical. This makes NTA still the favorite option for exosomes quantification, despite the limitations described above. In this case, NTA is considered appropriated to normalize the fluorescence intensity and the subsequent uptake experiments as the data, even though not perfect, give a sufficiently accurate readout. Moreover, from the data obtained on NTA density, it is clear that this technique was able to detect EQ higher particle concentration, that is consistent with the data obtained in AFM. Still, when discussing results, we still took into consideration the possibility that NTA underestimates EQ preparations, due to the instrument limits, but the discrepancy is mitigated by the CD9 data obtained. The results are resumed in Table 4.6.

Table 4.6 EQ preparations show less fluorescence intensity associated to the exosomal marker CD9. Data are from an ELISA assay on equal number of particles based on the NTA measurements from table 2. Values are expressed in arbitrary units (a.u.) as the average fluorescence intensity ± standard deviation as well as p values on data acquired in triplicate.

		Fluorescence intensity/ billion particles (a.u.)	
GASC	**EQ**	207 ± 74	*p=0.0099*
	UC	473 ± 67	
A172	**EQ**	471 ± 136	*n.s.*
	UC	542 ± 104	

Interestingly, EQ samples show less fluorescence CD9-associated, and especially in GASC preparations. This result is contrary to the previous results that state the higher amount of particles isolated with EQ method, thus suggesting that probably this latter, compared to UC, precipitates particles that are not all CD9 positive.

The CD9 ELISA assay somehow demonstrates that the huge amount of small particles in EQ preparations, not detected in NTA, do not correlate with a broad increase of CD9-

positive particles. Conversely, it seems that, when normalized to NTA particle count, CD9 is more expressed in UC-isolated samples. This data is more relevant for GASC supernatants.

Together the results imply that the NTA quantification method is fairly reliable among the used methods in estimating the exosomal content of a preparation.

This statement is peculiarly true in case of A172, as the CD9/number of particles ratio is comparable for UC and EQ samples, hinting that the small EQ particles that are not detected in NTA, do not alter the CD9 content of the preparations. Regarding GASC culture media EQ purified exosomes show less CD9 positive particles, suggesting a lower exosomal content.

Anyway we can safely say that even though NTA possibly underestimates the amount of particles (especially for EQ samples), it does not underestimate the number of exosomal amount.

4.4 A172 CELLS PREFERENTIALLY UPTAKE PARTICLES PURIFIED BY EXOQUICK PRECIPITATION

Once we assessed the effects of EQ and UC isolation methods on size distribution and particle concentration, we decided to evaluate how the different particle size affected the cellular uptake. To perform the internalization assays, we labelled the particles with a lipophilic dye, namely DiD, and conditioned approximately 20,000 A172 cells with $0.5x10^9$ NTA-counted labelled exosomes. Images were taken on live cells at 1, 3, and 6 hours, confirming the actual internalization for both preparations, but in different amounts. In fact, as shown in Figure 4.8 and 4.9, we discovered that either GASC- or A172- EQ isolated particles extensively entered A172 cells within 3 hours, while UC preparations needed 6 hours for a significant uptake.

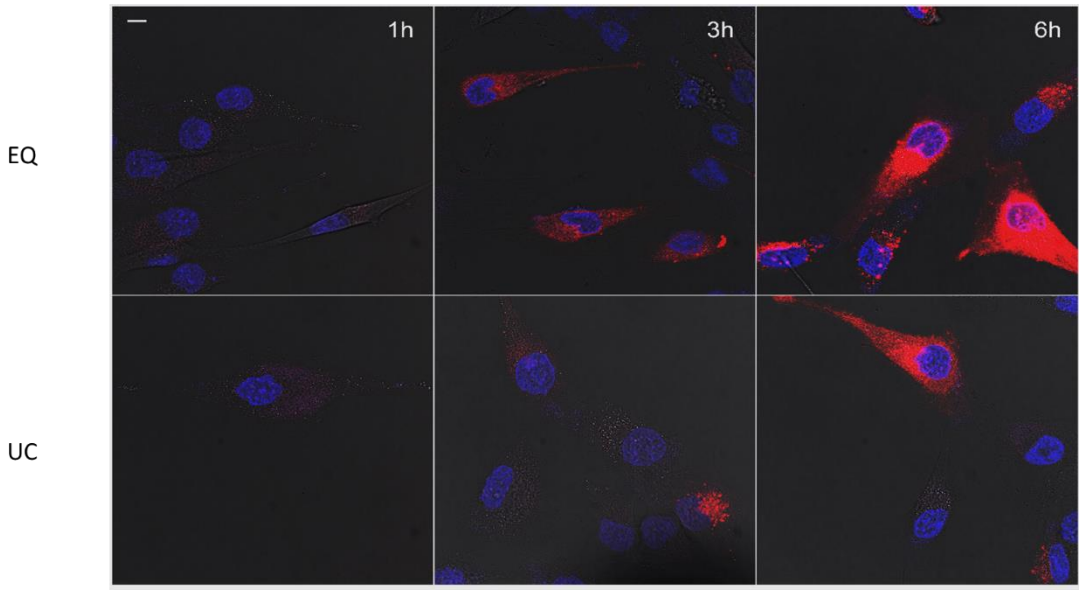

Figure 4.7 Internalization assay preformed on A172 cells (blue: Hoechst nuclear staining) by EQ- (upper images) and UC- (bottom images) DiD labelled (red fluorescence) GASC exosomes. The images represent the overlaid channels of the two emissions. Scale bar is 10 µm.

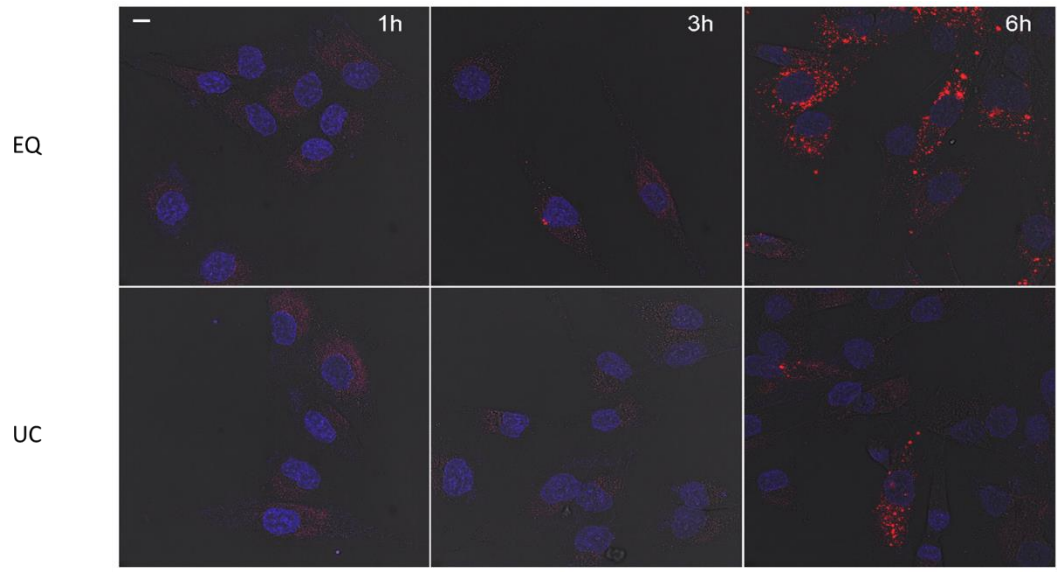

Figure 4.8 Internalization assay preformed on A172 cells (blue: Hoechst nuclear staining) by EQ- (upper images) and UC- (bottom images) DiD labelled (red fluorescence) A172 exosomes. The images represent the overlaid channels of the two emissions. Scale bar is 10 µm.

Moreover, GASC exosomes appear to be internalized more efficiently than A172 exosomes.

To further support the higher uptake of EQ isolated particles, FACS analyses were preformed to assess the mean fluorescence intensity (MFI) of DiD labelling on A172 cells. The results, shown in Figure 4.10 and 4.11, confirmed the data obtained by

confocal imaging, corroborating the concept that A172 cells preferentially uptake EQ-precipitated exosomes (from either GASC or A172 supernatants) rather than UC-precipitated exosomes.

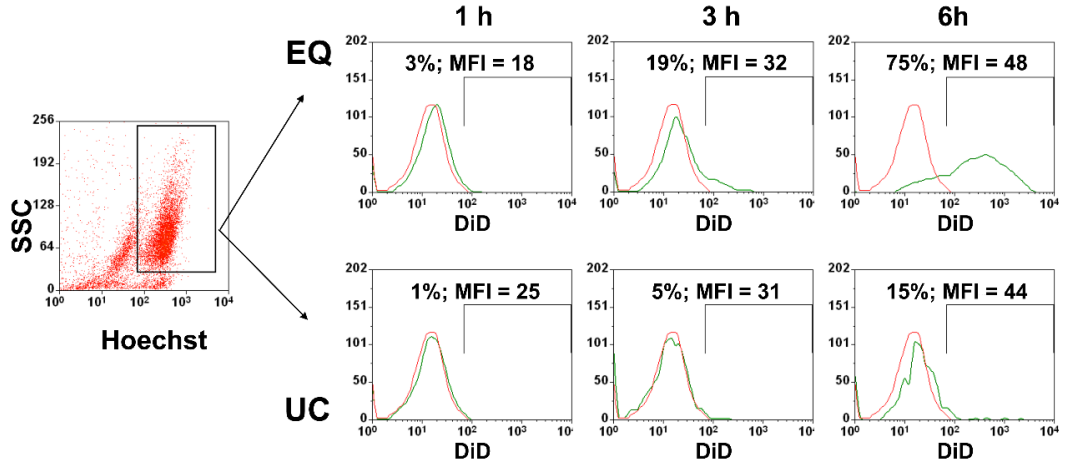

Figure 4.9 Flow cytometry analyses of the uptake of GASC exosomes by A172 cells. On the left, a representative plot showing the Hoechst-positive population (gated) assessed for DiD presence. On the right, histograms showing DiD expression of A172 cells conditioned, for different times, by EQ isolated exosomes (upper three panels at 1, 3 and 6 hours) and UC precipitated exosomes (lower three panel at 1, 3 and 6 hours). The histograms overlay non-conditioned A172 cells (red) and GASC exosomes-conditioned A172 cells (green). In each plot it is indicated the percentage of the DiD-Hoechst double positive cells and the relative mean fluorescence intensity ratio (MFI).

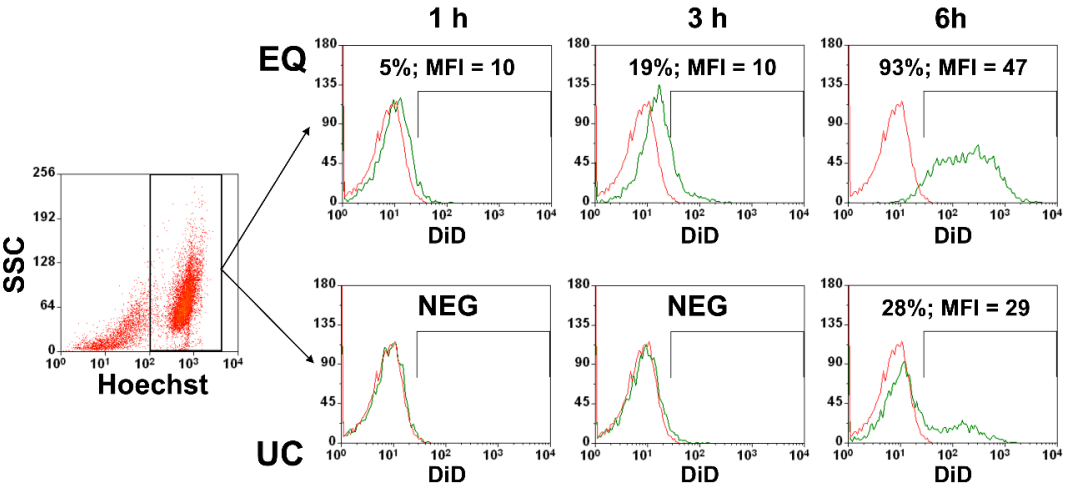

Figure 4.10 Flow cytometry analyses of the uptake of A172 exosomes by A172 cells. On the left, a representative plot showing the Hoechst-positive population (gated) assessed for DiD presence. On the right, histograms showing DiD expression of A172 cells conditioned, for different times, by EQ isolated exosomes (upper three panels at 1, 3 and 6 hours) and UC precipitated exosomes (lower three panel at 1, 3 and 6 hours). The histograms overlay non-conditioned A172 cells (red) and A172 exosomes-conditioned A172 cells (green). In each plot it is indicated the percentage of the DiD-Hoechst double positive cells and the relative mean fluorescence intensity ratio (MFI).

Moreover, to further assess if the uptake could reach, for EQ and UC preparations, a saturation point over longer times, A172 cells were incubated with DiD-labelled GASC exosomes for intervals of time that ranged from 1 to 72 hours. The results are reported in Figure 4.12a and 4.12b. The analysis showed that even if at 72 hours the fraction of DiD-positive cells were comparable for both EQ and UC exosomes, the first ones were already highly internalized at 6, 24 and 48 hours. This data could imply a different mechanism of uptake for the different isolated exosomes.

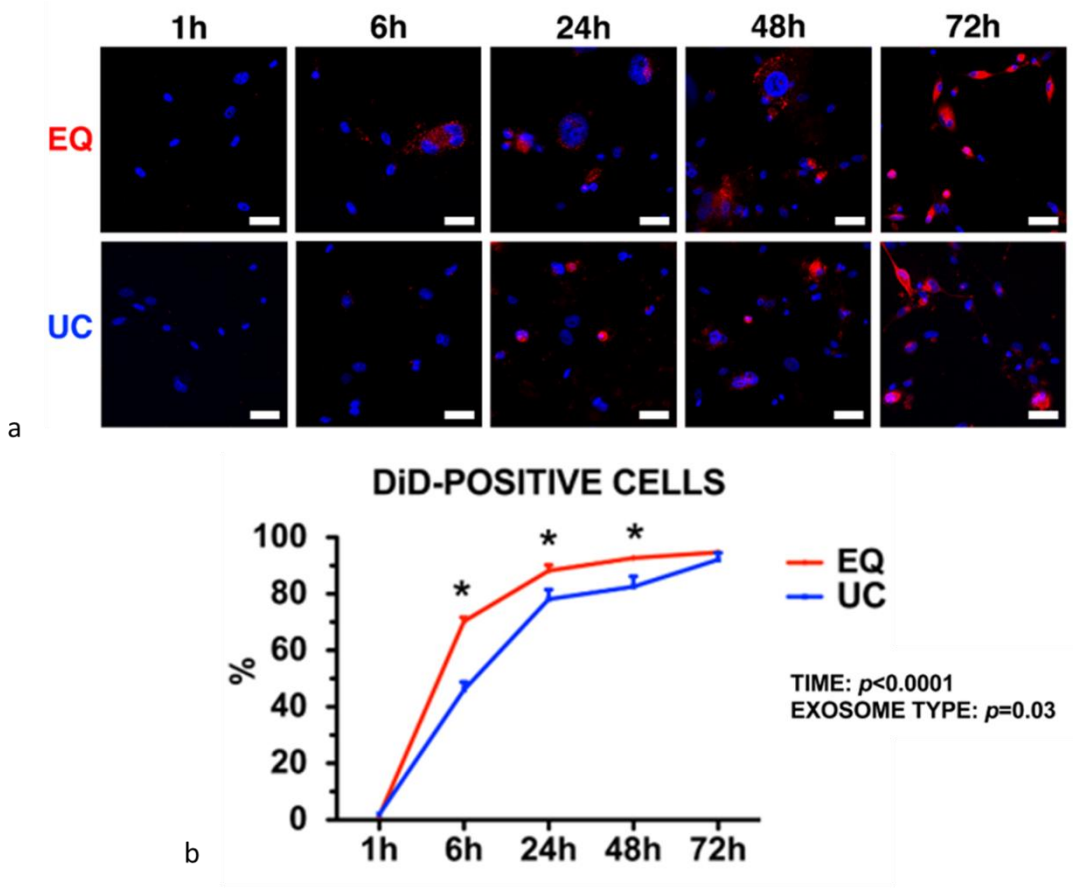

Figure 4.11 Kinetic of exosome uptake. Although EQ and UC exosomes seemed to reach a saturation at 72 hours, the uptake kinetic was different in the two preparations. (a) Internalization assay preformed on A172 cells (blue: Hoechst nuclear staining) with EQ- (upper images) and UC- (bottom images) GASC exosomes labeled by DiD (red fluorescence). Scale bar is 50μm. (b) Quantitative analysis of the DiD positive A172 cells (%) exposed to EQ- (red) and UC- (blue) exosomes, respectively. Data are displayed as mean ± standard deviation and p<0.05 (*) is calculated for EQ values versus UC ones.

To exclude the hypothesis that EQ preparations showed a higher fluorescence intensity due to an increased affinity of the DiD dye to EQ rather than UC, fluorescence intensity was quantified for both the preparations. Interestingly, we found that DiD fluorescence was less intense in EQ preparations, as reported in Table 4.7. These data proved that the

increased fluorescence intensities observed in A172 cells exposed to EQ-extracted exosomes were most likely due to increased uptake levels, rather than to increased intensities of the particles. To summarize, EQ isolated particles are less prone to be labelled by DiD, therefore it is unlikely that their preferential uptake by A172 cells could be the result of a more intense labelling.

Table 4.7 NTA-counted exosomal yield before and after DiD labelling and DiD fluorescence intensity of $1*10^9$ EQ and UC exosomes isolated both from GASC and A712. Data suggested that EQ preparations were less prone to labeling compared to UC. Moreover, the labelling procedure, no matter the source or the isolation method, determined a 90% loss of particles (comparing the first and the second column). Moreover, A172 exosomes seemed to be less DiD labelled, hinting a different vesicles' composition.

		NTA density before labelling (particles/ml)	**NTA density after labelling (particles/ml)**	**Fluorescence intensity/billion particles (a.u.)**
GASC	**EQ**	$3.1x10^{10}$	$3.9x10^{9}$	$1.19x10^{-6}$
	UC	$1.9x10^{10}$	$2.6x10^{9}$	$4.05x10^{-6}$
A172	**EQ**	$5.2x10^{10}$	$9.7x10^{9}$	$1.43x10^{-7}$
	UC	$2.6x10^{10}$	$4.5x10^{9}$	$1.90x10^{-7}$

As previously discussed, despite the inability of NTA to detect the total exosomal fraction, we could safely assume that, considering the ELISA assay, the amount of exosomes in the EQ preparations does not considerably varies from the putative one billion exosomes used for the uptake assays. On the other hand, the measurements seems acceptably accurate for UC samples.

To further assess whether the enhanced uptake of EQ preparations was size-dependent, we re-precipitated EQ-isolated A172 exosomes by UC, followed by DiD labelling. As previously assessed, the size distribution shifted from 50nm to nearly 100nm, compatibly with the data obtained in Table 4.4. Compared to the EQ precipitated control, the uptake of UC re-precipitated EQ exosomes was sensibly diminished, as shown in Figure 4.13. These evidences hint the possibility that ultracentrifugation somewhat operated a selection of the bigger particles and that deeply affected the cellular uptake of exosomes.

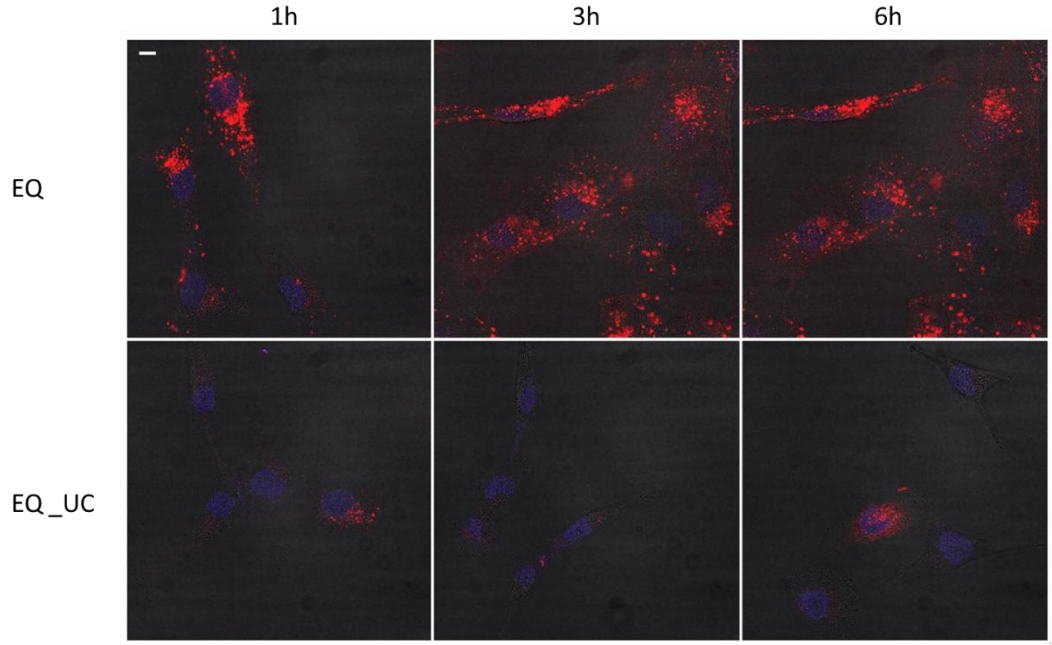

Figure 4.12 Uptake assay on A172 cells (blue: Hoechst nuclear staining) of EQ (upper three images) and EQ exosomes that underwent a consequential UC (bottom three images). Exosomes were labelled using DiD (red fluorescence). As shown, the internalization largely decreased upon re-precipitation of EQ exosomes using UC. Scale bar is 10 μm.

To rule out the possibility that ExoQuick itself could interfere with the internalization outcome observed, UC extracted exosomes were further precipitated by EQ and labeled by DiD. The images obtained in the uptake assay demonstrated that EQ precipitation did not increase the uptake of UC extracted exosomes, being this latter comparable to the UC precipitated control.

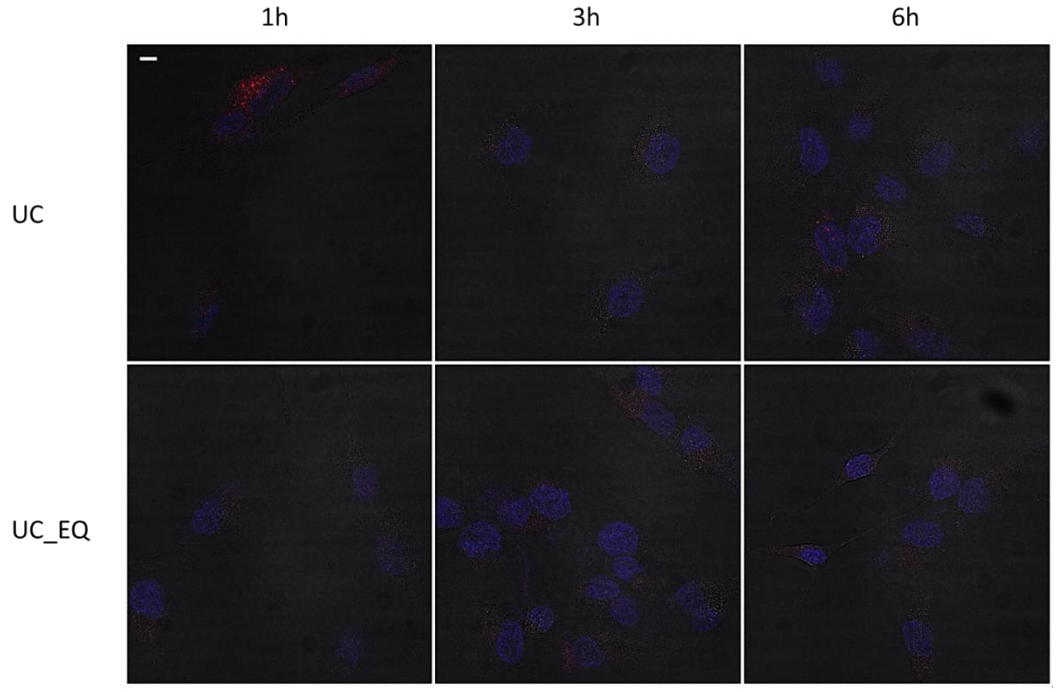

Figure 4.13 Uptake assay on A172 cells (blue Hoechst nuclear stained) of UC (upper three images) and UC exosomes that underwent a consequential EQ precipitation (bottom three images). Exosomes were labelled using DiD (red fluorescence). As shown, the internalization was not improved upon re-precipitation of UC exosomes using EQ. Scale bar is 10 µm.

Furthermore, to exclude that the increased uptake of EQ exosomes coud be due to the serum proteins co-precipitated with exosomes by EQ (Table 4.5 and Figure 4.7), we decided to assess the internalization of UC precipitated exosomes resuspended in EQ-precipitated PBS buffer and culture media. Results suggested, as displayed in Figure 4.15, that the protein component in the EQ precipitation did not increase the internalization of UC precipitated particles.

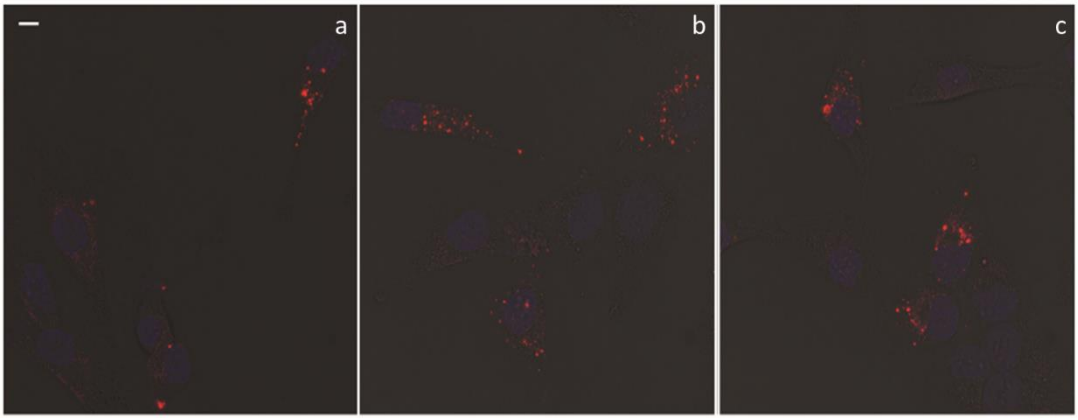

Figure 4.14 EQ medium protein precipitation did not affect the A172 exosomes' uptake by A172 cells. DiD is comparable in case of UC precipitated exosomes (a), and UC exosomes resuspended in EQ precipitated culture medium (b) or PBS buffer(c). Scale bar is 10 µm.

All the results obtained supported the hypothesis that A172 cells preferentially internalize EQ extracted exosomes and that this could be attributed to the small size of the EQ extracted particles. Thus, the uptake kinetics of exosomes is indirectly affected by the isolation method, as different purifications lead to preparations characterized by different particle size distributions.

4.5 THE EFFECTS OF EXOSOMES' DIFFERENTIAL UPTAKE ON FUNCTIONAL ASSAYS

We previously showed that A172 cell cultures increase their motility rate when conditioned with GASC exosomes [37]. Therefore, we decided to assess if EQ- and UC-extracted exosomes could induce different functional behaviors in A172 cell cultures.
We exposed to $0.5x10^9$ NTA-counted EQ and UC GASC exosomes the same number of cells and we performed a scratch assay. In this assay, we scratched a confluent cell culture, making an incision and measuring the velocity at which the edges of the gap come together through time (μm/h). Figure 4.16 shows, through the images taken at 0, 6, 12, and 24 hours, that A172 cells incubated with EQ-purified exosomes have a higher motility (as they fill the incision quicker) with those conditioned with UC extracted exosomes compared to those not exposed to exosomes (control).

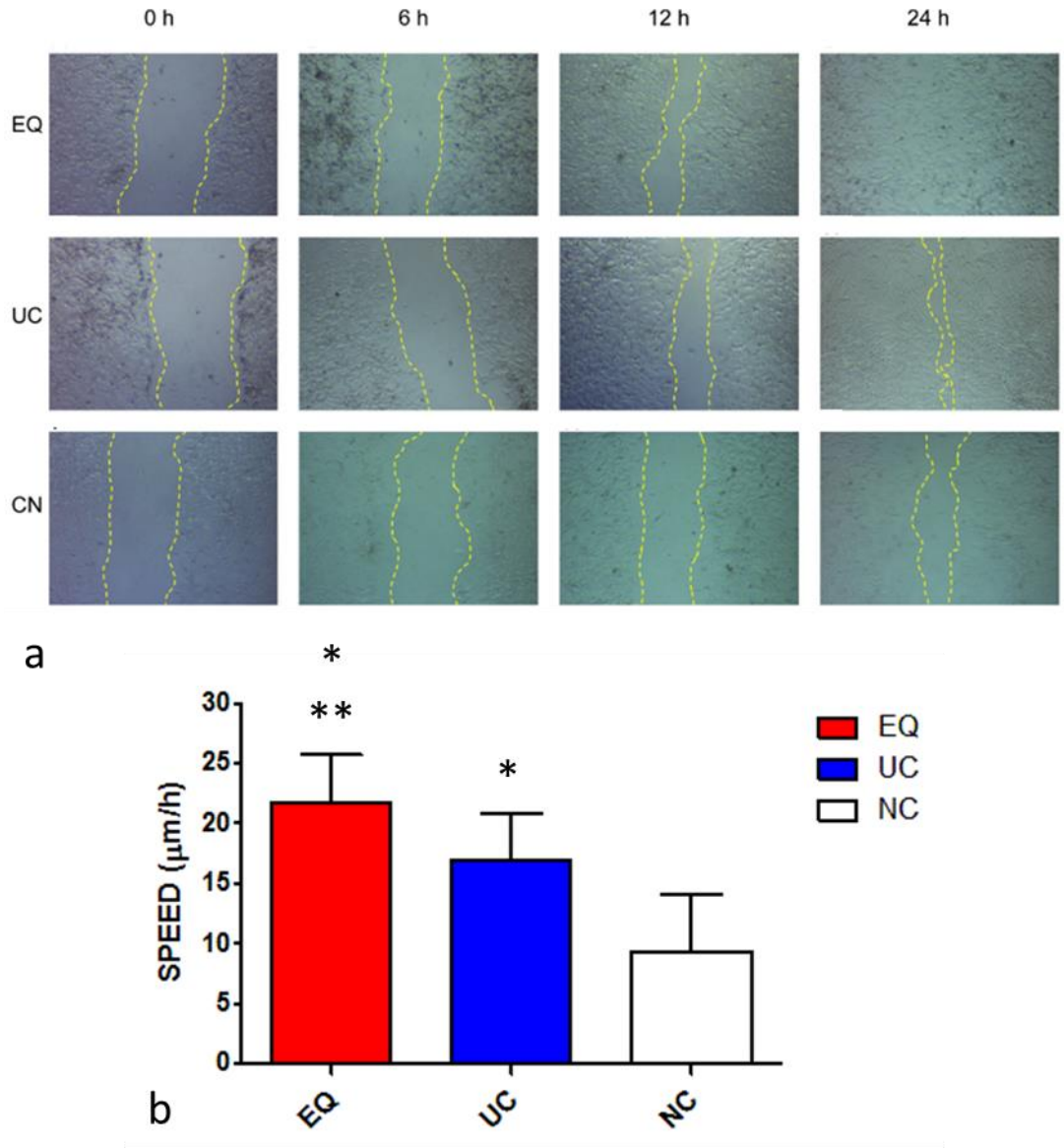

Figure 4.15 A172 conditioned by EQ extracted GASC exosomes displayed an improved motility compared to those conditioned by UC exosomes. Panel a shows representative images of the assay performed. Top four images show the motility of A172 cells exposed to EQ exosomes at different times. Middle four images show A172 cells exposed to UC exosomes. The bottom four images represent A172 cells that were not incubated with exosomes (Negative Control). Speed was calculated within the 12 hours and panel b shows the results as mean and standard deviation obtained from four replicates., p<0.05 vs. the negative control (NC).*

To further verify if the functional effects detected could be associated with the concentration of exosomes used for the conditioning, we performed further experiments with A172 cells exposed to different amounts of exosomes, from 10 times the one described in Figure 4.16, to amounts 10,000 times diluted. Figure 4.17 supported the existence of a possible dose-dependent effect of UC and EQ-extracted exosomes.

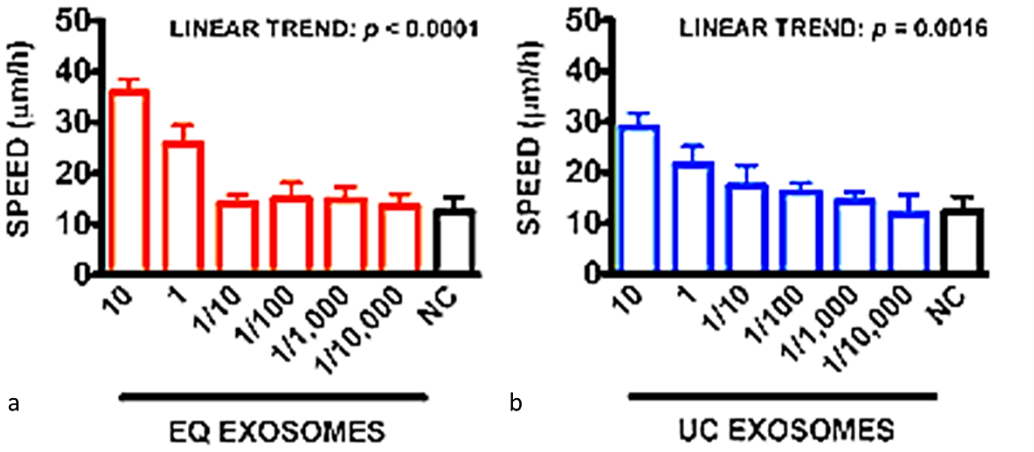

Figure 4.16 Motility assay results of the exosome concentration dilution, from 10 times higher to 10.000 times lower. Speed is calculated within the 24 hours, as for the previous experiment. The bar charts represents the mean and standard deviation obtained from three replicates. p values are calculated for the linear trend of dilutions.

These results imply that not only the EQ preparations showed an increased uptake kinetic, but also that this phenomenon is correlated to an improved functionality of the conditioned cell culture. Moreover, the increase of speed and the effectiveness of the delivering of the "message" is likely dose-dependent.

5 DISCUSSION

This thesis highlights the relevance of dissecting the morphological and physical features of exosomal samples instead of lingering on mere molecular characterizations. This topic earned much interest as exosomes are known as key players in the intercellular communication and they could be used in therapy as efficient nanocarriers [64].

Considering drug delivery systems, many different types of synthetic nanoparticles have been realized for this purpose, such as carbon, polymeric or metal nanoparticles, that upon different nanobioengineering have been functionalized to be internalized by target cells and deliver specific molecular signals [58]. Moreover, Shang et al. demonstrated that the uptake process was strongly influenced by the nanoparticle diameter, and defined, for many different cell cultures, the optimal diameter as the one ranging from 40nm to 50nm [58]. Although this aspect could have important clinical consequences, it has never been investigated, at least to our knowledge, for EVs.

For this reason, we characterized exosomes isolated using two different isolation methods, firstly focusing on the exosomal size, as EV diameter could deeply affect the way nanovesicles are internalized thus altering the functional asset of the recipient cells [88]. It is important to point out that this work did not study the mechanisms of exosome uptake by cells, though this could be an interesting future perspective.

In order to assess the size distribution of the UC and EQ-extracted GASC and A172 exosomes, we decided to use an optical (NTA) and a non-optical method (AFM). Our findings suggested that NTA, despite its wide use to estimate the particle concentration of exosomal preparations, lacks in establishing the accurate size distribution of the sample as it fails in detecting smaller particles. This was particularly evident in the EQ preparations, highly enriched in small particles, as assessed by AFM. In literature, it has been widely recognized that the NTA detection technique gives poor results in estimating the number of biological and lipid particles with a diameter inferior to 50nm, probably because of their low scattering intensities [81]. DLS was also employed as an optical method to quantify exosomal preparations but, as for the NTA, it requires extremely selected preparations, in terms of both purity and polydispersity, as non-exosomal debris or protein aggregates could affect the scattering measurements. Despite these quantification method resulted in inaccurate results, a deeper morphological

estimation was possible using AFM. This technique, even if extremely time-consuming and expensive, was able to detect the size of the particles, based on the height profile that corresponds to the diameter of the particle attached to the mica surface. It is possible, though, that there could occur some isovolumetric deformation, as the particle adheres to the mica and thus not appearing perfectly spherical. This phenomenon has already been reported in various articles [38,81,89–91], but it depends on the preparation and analysis setting applied. However, especially for UC preparations, AFM measurements seemed to be comparable to the ones obtained using other detection approaches, convincing us that the setting we used to analyze the particles lead to a minimal deformation and an optimal accuracy, thus assuming a spherical shape. Furthermore, it is important to point out that AFM is very different from NTA and DLS. These latter, in fact, are very sensitive to parameters such as temperature or viscosity of the fluid, and they are taken into consideration to estimate the hydrodynamic diameter, the key computed algorithm given as read-out. AFM, on the other hand, is less perturbed by the environmental conditions, as the measurements are carried out in a "dry state".

Regarding exosomes shape, AFM analyses revealed a heterogeneous scenario. Although most measurements confirmed for exosomes a spherical-like shape, some of them resulted irregular. This phenomenon could be due to the fact that the tip size (4nm in average) lead to the inability to systematically study the exosomal shape.

Considering the size distribution, we observed significant differences related to the isolation method, being EQ preparations, with respect to the UC ones, characterized by smaller size. This concept has been widely discussed by Gardiner et al., who reported an ISEV position paper treating, among other subjects, the diverse results obtained by adopting different isolation and quantification procedures [83]. The article stated that, even though no gold standard in both processes is in place, it is important to carefully describe the procedures applied, as different isolation or quantification techniques could deeply affect the results obtained. Moreover, differences in the particle size can reflect the quantification method, such as the hydrodynamic diameter for NTA or AFM slightly deformed dry state diameter and the conditions in which EVs are measured. About this, Dominguez-Medina et al. reported an increase of the hydrodynamic diameter of about 10nm caused by the proteins present in the serum that could form a "corona" that, surrounding the particles, could result in a raise in diameter [92].

For its detection limit (50nm), NTA is not ideal for the estimation of the particle concentration either. However, estimating the exosome amount by molecularly assessing CD9, an exosome specific marker, we established that NTA did not significantly underestimate the exosomal fraction in the EQ samples, being CD9 signal lower than that observed in the analogous NTA-counted UC particles. On the other hand, evidences report that different subsets of exosomes can differ in the amount of specific tetraspanins and we cannot exclude that this is the case of our experimental setting too[87].

Nevertheless, NTA has been found to be much more accurate in defining the exosomes density than methods based on the quantification of the protein content. As a matter of facts, we observed that chemical-precipitated preparations were contaminated by huge amounts of serum proteins, thus challenging the quantification of these samples. As this is a very crucial problem in the extracellular vesicles scenario, as polymeric precipitations are more and more used for exosome purification, many commercial kits are now available to evaluate exosome-specific protein markers, such as CD9, CD63 and CD81. This is a very attractive approach, as it would not only detect different subpopulations in the same preparation but also, as in our case, combined with an optical method such as NTA, would permit to avoid the overestimation of the exosomes by excluding non-exosomal vesicles possibly present in the preparations. However, it is important to highlight that the molecular approach could be applied only when comparing the same sources of exosomes, as assuming that every source retain the same amounts of each exosomal markers would be misleading.

Our revealing results indicate that different isolation methods lead to particles that differ in terms of size distribution and that this distinction was possible using AFM. In detail, the particles isolated using EQ purification appeared smaller than the particles isolated from the same source but precipitated using ultracentrifugation. At first, these data were not paralleled by differences in morphology and CD9 content of the different exosomes preparations, but they were enlightening when we proceeded with the cellular uptake experiments. In fact, exosomes isolated from the same GASC supernatants by different methods, displayed different uptake kinetics, as EQ-extracted exosomes seemed to be internalized faster than the UC-precipitated ones. Performing various controls, such as double precipitations and checking the contribution of serum proteins and aggregates in EQ samples, we reached the conclusion that the effect revealed was associated with the size distribution of the particles

In order to assess if the size-dependent internalization phenomena was restricted to the exosomal source (GASC), we performed the same experiments using A172 EQ- and UC-precipitated exosomes. The results obtained confirmed the size dependent cell uptake of exosomes, supporting the notion that the event was not cell type-specific.

Literature reported a huge amount of articles studying the impact of isolation methods on the extraction yield, morphological features and the biological properties of the exosomes [53,59,76,77,85]. Zlotogorski-Hurvitz et al. studied exosomes from UC and EQ preparations isolated from saliva and found that UC exosomes were smaller than EQ, besides different morphology as well as molecular features [85]. On the other hand, an article reported an increased size of UC exosomes when compared to density gradient precipitated particles [76,93]. Density gradient precipitation has been described as an efficient and accurate method for the study of the downstream RNA cargo of the exosomes, although it is delineated by lower yields in terms of particles, when compared to UC and EQ [59]. Although recent literature has described in detail the differences between isolation methods, no information are available on the effects on the uptake of exosomes by the recipient cells, with the exception of Franzen's group that studied the kinetic of uptake of UC exosomes by gall bladder cancer cells [60]. To our knowledge, this is the first study that compares the cell uptake of exosome preparations obtained by two different isolation method, and assesses the effects of the differential exosome uptake on cell motility.

Our results suggested that the isolation method profoundly impact the size distributions of the exosomal preparations and that this was associated with differences in the uptake and functional abilities of isolated exosomes. Conversely to the nanoparticles described by Shang et al. in which size was the only property affecting cell uptake, it would be incorrect to expand this knowledge to exosomes [58]. In fact, it could be possible that the different exosomes populations isolated by EQ and UC could differ not only in size, but also in other features, such as electrochemical membrane potential, surface proteins or molecular cargos, and that the functional effects observed could be the result of these differences. Still, our data imply that size deeply affects uptake kinetics and thus the biological functions of the receiving cells.

Considering this work, EQ precipitation has been revealed as the best isolation method, when studying cell uptake kinetics. Indeed, small EQ-exosomes are internalized faster than large UC-exosomes, thus leading to an enhanced functional effect (cell motility) on

the recipient cells. On the contrary, EQ samples are recognized as a highly impure preparation, due to the isolation method that tends to precipitate proteins or non-exosomal aggregates and as their size could be comparable to the small EQ precipitated exosomes, an accurate characterization is rather challenging.

Concerning uptake, an important path to investigate would be the internalization mechanisms and whether they are different depending on exosomes size or exosomes isolation methods. Many articles reported a wide range of mechanisms of entrance of exosomes, such as membrane fusion or clathrin-dependent/independent endocytosis [57,78]. Our laboratory is actually focusing on the mechanisms of entrance of exosomes, trying to assess the contribution of each singular pathway to the cumulative exosomal uptake.

Besides these considerations, our experiments suggest that cells preferentially uptake smaller exosomes that, as they are endowed with increased internalization kinetics, are able to trigger and enhanced functional response. This knowledge has a strong impact on possible exosome-involving therapies. In fact, it could be useful to use the size parameter to select exosomal subpopulations for therapeutic use. It would also be extremely interesting to study exosomes produced by different cell types in terms of size, to better understand their contribution to the recipient cell in terms of functional abilities. Based on the results reported, it would seem that cells producing smaller exosomes would be the more effective cells in shaping the microenvironment, resulting more efficient in delivering their message, compared to large-exosomes producing cells. GASC exosomes indeed have already been proved as key players in the support of tumor progression. Still, the involvement of size as a parameter to take into consideration for the effects obtained has not been investigated yet. Some authors, currently studying this subject, observed a difference in exosomal size distribution between normal and pathological cells [90]. There are still some main topics to further explore, such as the capacity of this differential uptake to trigger a significantly different response based on the physiological status of the producing cells. Systematic studies on different sizes observe in different cell types, their ability to promote different cellular responses would be extremely interesting as a future perspective, and it could take hint from the observations retrieved.

6 BIBLIOGRAPHY

1. Weathers, SP & Gilbert, MR. Advances in treating glioblastoma. *F1000Prime Rep* **6,** 46 (2014).

2. Louis, D. N. *et al.* The 2016 World Health Organization Classification of Tumors of the Central Nervous System: a summary. *Acta Neuropathol.* **131,** 803–20 (2016).

3. Bovenberg, M., Degeling, M. & Tannous, B. Advances in stem cell therapy against gliomas. *Trends Mol Med* **19,** 281–91 (2013).

4. Plate, K. H., Scholz, A. & Dumont, D. J. Tumor angiogenesis and anti-angiogenic therapy in malignant gliomas revisited. *Acta Neuropathol.* **124,** 763–75 (2012).

5. Chen, F. *et al.* New horizons in tumor microenvironment biology: challenges and opportunities. *BMC Med* **13,** 45 (2015).

6. Charles, NA, Holland, EC, Gilbertson, R, Glass, R & Kettenmann, H. The brain tumor microenvironment. *Glia* **59,** 1169–80

7. Codrici, E., Enciu, A.-M. M., Popescu, I.-D. D., Mihai, S. & Tanase, C. Glioma Stem Cells and Their Microenvironments: Providers of Challenging Therapeutic Targets. *Stem Cells Int* **2016,** 5728438 (2016).

8. Maher, E. A. *et al.* Malignant glioma: genetics and biology of a grave matter. *Genes Dev.* **15,** 1311–33 (2001).

9. Masui, K., Mischel, P. S. & Reifenberger, G. Molecular classification of gliomas. *Handb Clin Neurol* **134,** 97–120 (2016).

10. Kalkan, R. The Importance of Mutational Drivers in GBM. *Crit. Rev. Eukaryot. Gene Expr.* **26,** 19–26 (2016).

11. Verhaak, R. G. *et al.* Integrated genomic analysis identifies clinically relevant subtypes of glioblastoma characterized by abnormalities in PDGFRA, IDH1, EGFR, and NF1. *Cancer Cell* **17,** 98–110 (2010).

12. Mandel, J. J. *et al.* Impact of IDH1 mutation status on outcome in clinical trials for recurrent glioblastoma. *J. Neurooncol.* (2016). doi:10.1007/s11060-016-2157-2

13. Mizoguchi, M. *et al.* Clinical implications of microRNAs in human glioblastoma. *Frontiers in oncology* **3,** 19 (2013).

14. Zhang, M., Ye, G., Li, J. & Wang, Y. Recent advance in molecular angiogenesis in glioblastoma: the challenge and hope for anti-angiogenic therapy. *Brain Tumor Pathol* **32,** 229–36 (2015).

15. Julka, P. K. *et al.* Postoperative treatment of glioblastoma multiforme with radiation therapy plus concomitant and adjuvant temozolomide : A mono-institutional experience of 215 patients. *J Cancer Res Ther* **9,** 381–6 (2013).
16. Stupp, R., Toms, S. A. & Kesari, S. Treatment for Patients With Newly Diagnosed Glioblastoma--Reply. *JAMA* **315,** 2348–9 (2016).
17. Soda, Y., Myskiw, C., Rommel, A. & Verma, I. M. Mechanisms of neovascularization and resistance to anti-angiogenic therapies in glioblastoma multiforme. *J. Mol. Med.* **91,** 439–48 (2013).
18. Sundar, S. J., Hsieh, J. K., Manjila, S., Lathia, J. D. & Sloan, A. The role of cancer stem cells in glioblastoma. *Neurosurg Focus* **37,** E6 (2014).
19. ALTANER & ALTANEROVA. Stem cell based glioblastoma gene therapy. *Neoplasma* **59,** 756–760 (2012).
20. Bexell, D., Svensson, A. & Bengzon, J. Stem cell-based therapy for malignant glioma. *Cancer treatment reviews* **39,** 358–65 (2012).
21. Bovenberg, Degeling & Tannous. Advances in stem cell therapy against gliomas. (2013).
22. Collins, FS & Varmus, H. A new initiative on precision medicine. *N Engl J Med* **372,** 793–5
23. Martin, M., Wei, H. & Lu, T. Targeting microenvironment in cancer therapeutics. *Oncotarget* (2016). doi:10.18632/oncotarget.9824
24. Haddow, A. Molecular repair, wound healing, and carcinogenesis: tumor production a possible overhealing? *Adv. Cancer Res.* **16,** 181–234 (1972).
25. Hanahan, D & Weinberg, RA. The hallmarks of cancer. *Cell* **100,** 57–70
26. Fidoamore, A. *et al.* Glioblastoma Stem Cells Microenvironment: The Paracrine Roles of the Niche in Drug and Radioresistance. *Stem Cells Int* **2016,** 6809105 (2016).
27. Allen, M. & Louise Jones, J. Jekyll and Hyde: the role of the microenvironment on the progression of cancer. *J. Pathol.* **223,** 162–76 (2011).
28. Hambardzumyan, D. & Bergers, G. Glioblastoma: Defining Tumor Niches. *Trends Cancer* **1,** 252–265 (2015).
29. Ostman, A. & Augsten, M. Cancer-associated fibroblasts and tumor growth--bystanders turning into key players. *Curr. Opin. Genet. Dev.* **19,** 67–73 (2009).
30. Valcz, G., Sipos, F., Tulassay, Z., Molnar, B. & Yagi, Y. Importance of carcinoma-associated fibroblast-derived proteins in clinical oncology. *J. Clin. Pathol.* **67,** 1026–31 (2014).

31. Pistollato, F. *et al.* Intratumoral hypoxic gradient drives stem cells distribution and MGMT expression in glioblastoma. *Stem Cells* **28,** 851–62 (2010).
32. Lathia, J., Heddleston, J., Venere, M. & Rich, J. Deadly Teamwork: Neural Cancer Stem Cells and the Tumor Microenvironment. *Cell Stem Cell* **8,** 482–485 (2011).
33. Liebelt, B. D. *et al.* Glioma Stem Cells: Signaling, Microenvironment, and Therapy. *Stem Cells Int* **2016,** 7849890 (2016).
34. Beltrami, AP *et al.* Multipotent cells can be generated in vitro from several adult human organs (heart, liver, and bone marrow). *Blood* **110,** 3438–46
35. Cesselli, D. *et al.* Role of tumor associated fibroblasts in human liver regeneration, cirrhosis, and cancer. *Int J Hepatol* **2011,** 120925 (2011).
36. Domenis, R *et al.* Adipose tissue derived stem cells: in vitro and in vivo analysis of a standard and three commercially available cell-assisted lipotransfer techniques. *Stem Cell Res Ther* **6,** 2
37. Bourkoula, E. *et al.* Glioma-Associated Stem Cells: A Novel Class of Tumor-Supporting Cells Able to Predict Prognosis of Human Low-Grade Gliomas. *Stem Cells* **32,** 1239–1253
38. Andolfi, L. *et al.* Investigation of adhesion and mechanical properties of human glioma cells by single cell force spectroscopy and atomic force microscopy. *PLoS ONE* **9,** e112582 (2014).
39. Bang, C. & Thum, T. Exosomes: New players in cell–cell communication. *The International Journal of Biochemistry & Cell Biology* **44,** 2060–2064
40. Skog, J. *et al.* Glioblastoma microvesicles transport RNA and proteins that promote tumour growth and provide diagnostic biomarkers. *Nat. Cell Biol.* **10,** 1470–6 (2008).
41. Lin, R., Wang, S. & Zhao, R. Exosomes from human adipose-derived mesenchymal stem cells promote migration through Wnt signaling pathway in a breast cancer cell model. *Molecular and cellular biochemistry* **383,** 13–20 (2013).
42. Raposo, G & Stoorvogel, W. Extracellular vesicles: Exosomes, microvesicles, and friends. *The Journal of Cell Biology* **200,** 373–383
43. Abels, E. & Breakefield, X. Introduction to Extracellular Vesicles: Biogenesis, RNA Cargo Selection, Content, Release, and Uptake. *Cell Mol Neurobiol* **36,** 301–312 (2016).
44. Yáñez-Mó, M. *et al.* Biological properties of extracellular vesicles and their physiological functions. *J Extracell Vesicles* **4,** 27066 (2015).

45. Johnstone, R. Exosomes biological significance: A concise review. *Blood cells, molecules & diseases* **36,** 315–21 (2006).
46. Mathivanan, S., Ji, H. & Simpson, R. J. Exosomes: Extracellular organelles important in intercellular communication. *Journal of Proteomics* **73,** 1907–1920
47. Sun, D. *et al.* Exosomes are endogenous nanoparticles that can deliver biological information between cells. *Advanced Drug Delivery Reviews* **65,** 342–347
48. Vlassov, A. V., Magdaleno, S., Setterquist, R. & Conrad, R. Exosomes: Current knowledge of their composition, biological functions, and diagnostic and therapeutic potentials. *Biochimica et Biophysica Acta - General Subjects* **1820,** 940–948
49. Lee, Y., Andaloussi, S. & Wood, M. Exosomes and microvesicles: extracellular vesicles for genetic information transfer and gene therapy. *Hum Mol Genet* **21,** R125–R134 (2012).
50. Xu, R., Greening, D., Zhu, H.-J., Takahashi, N. & Simpson, R. Extracellular vesicle isolation and characterization: toward clinical application. *J Clin Invest* **126,** 1152–1162 (2016).
51. Atay, S. & Godwin, A. Tumor-derived exosomes. *Commun Integr Biology* **7,** e28231 (2014).
52. Record, M., Subra, C., Silvente-Poirot, S. & Poirot, M. Exosomes as intercellular signalosomes and pharmacological effectors. *Biochem Pharmacol* **81,** 1171–82 (2011).
53. Lässer, C., Eldh, M. & Lötvall, J. Isolation and characterization of RNA-containing exosomes. *Journal of visualized experiments : JoVE* e3037 doi:10.3791/3037
54. Johnsen, K. *et al.* A comprehensive overview of exosomes as drug delivery vehicles — Endogenous nanocarriers for targeted cancer therapy. *Biochimica et Biophysica Acta (BBA) - Reviews on Cancer* **1846,** 75–87 (2014).
55. Mathivanan, S., Fahner, C. J., Reid, G. E. & Simpson, R. J. ExoCarta 2012: database of exosomal proteins, RNA and lipids. *Nucleic Acids Research* **40,** D1241–4
56. Suntres, Z. E. *et al.* Therapeutic Uses of Exosomes. *Exosomes Microvescicles* **1,** 1–8 (2013).
57. Mulcahy, L. A., Pink, R. C. & Carter, D. R. Routes and mechanisms of extracellular vesicle uptake. *J Extracell Vesicles* **3,** (2014).
58. Shang, L., Nienhaus, K. & Nienhaus, G. U. Engineered nanoparticles interacting with cells: size matters. *J Nanobiotechnology* **12,** 5 (2014).
59. Deun, V. The impact of disparate isolation methods for extracellular vesicles on downstream RNA profiling. *Journal of extracellular vesicles* **3,** 1–14

60. Franzen, C. A., Simms, P. E. & Huis, V. Characterization of uptake and internalization of exosomes by bladder cancer cells. *BioMed research international* **2014,** 619829

61. Pitt, J. M. *et al.* Dendritic cell-derived exosomes for cancer therapy. *J. Clin. Invest.* **126,** 1224–32 (2016).

62. Février, B. & Raposo, G. Exosomes: Endosomal-derived vesicles shipping extracellular messages. *Current Opinion in Cell Biology* **16,** 415–421 (2004).

63. Azmi, AS, Bao, B & Sarkar, FH. Exosomes in cancer development, metastasis, and drug resistance: a comprehensive review. *Cancer Metastasis Rev* doi:10.1007/s10555-013-9441-9

64. Van den Boorn, J. G., sler, J., Coch, C., Schlee, M. & Hartmann, G. Exosomes as nucleic acid nanocarriers. *Advanced Drug Delivery Reviews* **65,** 331–335

65. Pant, S., Hilton, H. & Burczynski, M. The multifaceted exosome: Biogenesis, role in normal and aberrant cellular function, and frontiers for pharmacological and biomarker opportunities. *Biochemical Pharmacology* **83,** 1484–1494 (2012).

66. Kosaka, N. *et al.* Exosomal tumor-suppressive microRNAs as novel cancer therapy 'Exocure' is another choice for cancer treatment. *Advanced Drug Delivery Reviews* **65,** 376–382 (2013).

67. Gajos-Michniewicz, A., Duechler, M. & Czyz, M. MiRNA in melanoma-derived exosomes. *Cancer Lett* **347,** 29–37 (2014).

68. Yu, B., Zhang, X. & Li, X. Exosomes Derived from Mesenchymal Stem Cells. *Int J Mol Sci* **15,** 4142–4157 (2014).

69. Al-Nedawi, K., Meehan, B. & Rak, J. Microvesicles: messengers and mediators of tumor progression. *Cell Cycle* **8,** 2014–8 (2009).

70. Li, C. C. *et al.* Glioma microvesicles carry selectively packaged coding and non-coding RNAs which alter gene expression in recipient cells. *RNA Biol* **10,** 1333–44 (2013).

71. Bing, Z.-T. T., Yang, G.-H. H., Xiong, J., Guo, L. & Yang, L. Identify signature regulatory network for glioblastoma prognosis by integrative mRNA and miRNA co-expression analysis. *IET Syst Biol* **10,** 244–251 (2016).

72. André-Grégoire, G. & Gavard, J. Spitting out the demons: Extracellular vesicles in glioblastoma. *Cell Adh Migr* 1–9 (2016). doi:10.1080/19336918.2016.1247145

73. D'Asti, E., Chennakrishnaiah, S., Lee, T. H. & Rak, J. Extracellular Vesicles in Brain Tumor Progression. *Cell. Mol. Neurobiol.* **36,** 383–407 (2016).

74. Saadatpour, L. *et al.* Glioblastoma: exosome and microRNA as novel diagnosis biomarkers. *Cancer Gene Ther.* (2016). doi:10.1038/cgt.2016.48

75. Gourlay, J. *et al.* The emergent role of exosomes in glioma. *J Clin Neurosci* (2016). doi:10.1016/j.jocn.2016.09.021

76. Tauro, B. J. *et al.* Comparison of ultracentrifugation, density gradient separation, and immunoaffinity capture methods for isolating human colon cancer cell line LIM1863-derived exosomes. *Methods* **56,** 293–304 (2012).

77. Schageman, J. *et al.* The complete exosome workflow solution: from isolation to characterization of RNA cargo. *BioMed research international* **2013,** 253957

78. Tian, T., Wang, Y., Wang, H., Zhu, Z. & Xiao, Z. Visualizing of the cellular uptake and intracellular trafficking of exosomes by live-cell microscopy. *Journal of Cellular Biochemistry* **111,** 488–496

79. Van der Pol, E *et al.* Particle size distribution of exosomes and microvesicles determined by transmission electron microscopy, flow cytometry, nanoparticle tracking analysis, and resistive pulse sensing. *Journal of Thrombosis and Haemostasis* **12,** 1182–1192

80. Van der Pol, E, Coumans, F, Varga, Z, Krumrey, M & Nieuwland, R. Innovation in detection of microparticles and exosomes. *Journal of thrombosis and haemostasis : JTH* **11 Suppl 1,** 36–45

81. Pol, V. Optical and non-optical methods for detection and characterization of microparticles and exosomes. *Journal of Thrombosis and Haemostasis* **8,** 2596–2607

82. Lotvall, J *et al.* Minimal experimental requirements for definition of extracellular vesicles and their functions: a position statement from the International Society for Extracellular Vesicles. *J Extracell Vesicles* **3,** 26913 (2014).

83. Gardiner, C. *et al.* Techniques used for the isolation and characterization of extracellular vesicles: results of a worldwide survey. *J Extracell Vesicles* **5,** (2016).

84. Unknown. Thery et al., Exosome Protocols (1).pdf.

85. Unknown. COMPARISON METODI.pdf.

86. Witwer, K. W. *et al.* Standardization of sample collection, isolation and analysis methods in extracellular vesicle research. *Journal of extracellular vesicles* **2,** 1–25

87. Hoen, E. N. *et al.* Quantitative and qualitative flow cytometric analysis of nanosized cell-derived membrane vesicles. *Nanomedicine: Nanotechnology, Biology, and Medicine* **8,** 712–720 (2012).

88. Simons, M. & Raposo, G. Exosomes–vesicular carriers for intercellular communication. *Current opinion in cell biology* **21,** 575–581

89. Sharma, S. *et al.* Structural-mechanical characterization of nanoparticle exosomes in human saliva, using correlative AFM, FESEM, and force spectroscopy. *Acs Nano* **4,** 1921–6 (2010).

90. Zlotogorski-Hurvitz, A., Dayan, D., Chaushu, G., Salo, T. & Vered, M. Morphological and molecular features of oral fluid-derived exosomes: oral cancer patients versus healthy individuals. *Journal of Cancer Research and Clinical Oncology* (2015). doi:10.1007/s00432-015-2005-3

91. Sharma, S., Das, K., Woo, J. & Gimzewski, J. K. Nanofilaments on glioblastoma exosomes revealed by peak force microscopy. *Journal of the Royal Society, Interface / the Royal Society* **11,** 20131150

92. Dominguez-Medina, S., McDonough, S., Swanglap, P., Landes, C. F. & Link, S. In situ measurement of bovine serum albumin interaction with gold nanospheres. *Langmuir* **28,** 9131–9 (2012).

93. Zhang, Z., Wang, C., Li, T., Liu, Z. & Li, L. Comparison of ultracentrifugation and density gradient separation methods for isolating Tca8113 human tongue cancer cell line-derived exosomes. *Oncology letters* **8,** 1701–1706 (2014).